Bulletin of Mathematical Biology (2009) 71: 2048–2079
DOI 10.1007/s11538-009-9457-z

ORIGINAL ARTICLE

Modeling Spatial Spread of Infectious Diseases with a Fixed Latent Period in a Spatially Continuous Domain

Jing Li[a,b], Xingfu Zou[a,*]

[a] *Department of Applied Mathematics, University of Western Ontario, London, ON N6A 5B7, Canada*
[b] *Department of Mathematics and Statistics, University of Ottawa, Ottawa, ON K1N 6N5, Canada*

Received: 12 November 2008 / Accepted: 30 March 2009 / Published online: 29 September 2009

Abstract In this paper, with the assumptions that an infectious disease in a population has a fixed latent period and the latent individuals of the population may diffuse, we formulate an SIR model with a simple demographic structure for the population living in a spatially continuous environment. The model is given by a system of reaction-diffusion equations with a discrete delay accounting for the latency and a spatially non-local term caused by the mobility of the individuals during the latent period. We address the existence, uniqueness, and positivity of solution to the initial-value problem for this type of system. Moreover, we investigate the traveling wave fronts of the system and obtain a critical value c^* which is a lower bound for the wave speed of the traveling wave fronts. Although we can not prove that this value is exactly the minimal wave speed, numeric simulations seem to suggest that it is. Furthermore, the simulations on the PDE model also suggest that the spread speed of the disease indeed coincides with c^*. We also discuss how the model parameters affect c^*.

Keywords Latent period · Diffusion · Traveling waves · Wave speed · Spread speed · Non-local infection

1. Introduction

Mathematical models have been extensively used to study the dynamics of infectious diseases in population level. Most continuous time models are in the form of ordinary differential equations (ODEs) (see, e.g., Brauer et al., 2008; Hethcote,, 2000). Such ODEs models assume that the population are well mixed, and the transmission are instantaneous. In reality, the environment in which a population lives is often heterogeneous making it necessary to distinguish the locations. Also, some diseases have a latency: infected

*Corresponding author.
E-mail addresses: jli333@uwo.ca (Jing Li), xzou@uwo.ca (Xingfu Zou).
Research supported by NSERC, by NCE-MITACS of Canada and by PREA of Ontario.

individuals do not infect other susceptible individuals until some time later. Taking the human tuberculosis or bovine tuberculosis as an example, it may take months for the infection to develop to the infectious stage (see, e.g., Anderson and Trewhella, 1985; Barlow, 2000; Garnett et al., 2002; Thoen et al., 1984 and references therein).

In order for a model to be more realistic, the above factors should be incorporated into the model. For the latter, in their recent work van den Driessche et al. (2007) set up an SEIR model with a general probability function $p(t)$ to account for the probability that an exposed individual still remains in the exposed class t time units after entering the exposed class. When $p(t)$ is subject to a negatively exponentially distribution, the model reduces to one still described by an ODEs system. The situation when $p(t)$ is a step function is more interesting. Indeed, when

$$p(t) = \begin{cases} 1, & 0 \le t \le \tau, \\ 0, & t > \tau, \end{cases}$$

where $\tau > 0$ can be explained as the average latent period of the disease, the model becomes a system of delay differential equations (DDEs) with the discrete delay τ. Such a DDEs system is much harder to analyze and may demonstrate richer dynamics such as oscillatory dynamics (see van den Driessche et al., 2007) which is common in reality.

For the factor of spatial heterogeneity, the environment can be spatially *discrete* or spatially *continuous*. In either case, a model has to contain terms that describe the mobility of the population. The concept of patch naturally arises in the spatially *discrete* case, and a patch can be a city, a town, a region, or even a country, depending on the context. For such a patch environment, the dispersal between patches may be due to travels and migrations. Along this line, there have been some works investigating the effects of population dispersal on disease dynamics. Arino and van den Driessche (2003a, 2003b, 2006) formulated epidemic models with populations traveling among cities in which the residences of individuals are maintained. Wang and Zhao (2004, 2005) considered epidemic models of multi-patches without tracking the residence of individuals. Wang and Zhao (2006) proposed an epidemic model with population dispersal and infection period. Salmani and van den Driessche (2006) discussed an SEIRS epidemic model on patches to describe the dynamics of an infectious disease in a population in which individuals travel between patches. Hsieh et al. (2007), Brauer and van den Driessche (2001), Castillo-Chavez and Yakubu (2001) and Wang and Mulone (2003) are also among studies of epidemic models of meta-populations.

When the environment is spatially continuous, random diffusion is often used to describe the mobility of the population, leading to models in the form of reaction diffusion equations (see, e.g., Brauer et al., 2008; Murray, 2002). For such partial differential equation models for infectious diseases, much less is done. On the other hand, from such models, there arise some very important and interesting mathematical and biological problems among which are traveling wave solutions and geographical spread speed of the disease. Results on these topics may help one predict how fast a disease invades geographically, and accordingly, take necessary measures in advance to prevent the disease, or at least, decrease possible negative consequences. It turns out that these topics are very challenging mathematical problems due to the nature of prey-predator type interaction of the model (see, e.g., Murray, 2002).

There arises the nature question: how to incorporate *both* factors into an ODEs disease model? Would it be reasonable or acceptable if one simply combines the models considered separately for these two factors as discussed above? In general, the answer is no, because if individuals disperse during the latent period, an individual infected at location A could be anywhere in the environment when he/she enters the infectious class. In other words, the rate of gaining infectious individuals at a location at the present time actually depends on the infections not only at this location but also at all other locations at previous times. For patch environments, in our recent work (Li and Zou 2009a, 2009b), by tracking the infection age and the mobility of latent individuals, we derived two models, one without demographic structure which is a generalization of the classic Kenmark–McKendrick model (see Li and Zou, 2009a), and the other with a simple demographical structure (see Li and Zou,, 2009b). Analysis and numeric simulations on these two models have given us some information on how the spatial dispersal and the length of latent period jointly affect the disease dynamics.

Incorporating these two factors into an SIR disease model in a spatially continuous environment constitutes the main purpose of this paper. Following the main idea in Li and Zou (2009a, 2009b) but using different techniques, we derive in Section 2, a new model which is in the form of reaction-diffusion equations with a *temporal delay* and a *non-local infection* term. The delay is exactly the latent period and the non-local term is due to the random diffusion of the latent individuals. In Section 3, by an abstract setting of the model system, we address the basic questions of existence, uniqueness, and positivity of solutions to the initial value problem associated with the model system. In Section 4, we explore traveling wave fronts of the model system that connect the disease free equilibrium and the unique endemic equilibrium. By analyzing the behavior of solutions to the wave equation near the disease free equilibrium, we find a critical value c^* which serves at least as a lower bound of speed for traveling wave fronts in the sense that any traveling wave front must have speed no less than c^*. The dependence of c^* on the model parameters are discussed preliminarily in Section 4 and then summarized in Section 6, which shows the joint impact of the diffusion rates and latency length on the spread speed. We perform some numeric simulations in Section 5 for both the wave equation and the original PDE system. The simulation results suggest that c^* is indeed the minimal wave speed and it is also actually the geographical spread speed of the disease. Unfortunately, we are not able to theoretically prove the above conjecture in this paper. This is mainly because of the nature of prey-predator type interaction, as well as the presence of both the time delay and the spatially non-local term in the model. Due to these, neither the method of monotone iteration coupled with upper-lower solutions developed in Wu and Zou (2001) for monotone delayed reaction diffusion systems, nor the methods used in Dunbar (1981, 1983, 1984), in Gardner (1984), and in Huang et al. (2003) can be applied. It is also the prey-predator type interaction that makes the system non-monotone and, therefore, the theory for asymptotic spread speed recently developed in Liang and Zhao (2007) fails to apply. All these leave some very challenging yet important open mathematical problems.

2. Model formulation

Consider an infectious disease that has a fixed period of latency, denote by τ. For some diseases, the latency is not fixed: it depends on individuals and is subject to some distrib-

utions. In such a situation, the assumption of a fixed length of latency can be considered as an approximation of the mean latency, but would simplify the model. Assume that the disease has full immunity after recovery (regardless of natural recovery or recovery due to treatments). Following the convention, the total population is divided into four classes: susceptible class, latent class, infectious class, and removed classed, with the sub-populations denoted by S, L, I, and R, respectively. Susceptible class consists of those individuals that can be infected; latent class includes those who have been exposed and infected by the disease but can not yet infect other susceptible individuals; infectious class consists of individuals capable of infecting others; and the removed class includes those who are fully out of the transmission chain, consisting of, e.g., the deaths, the recovered ones with full immunity, and possibly isolated individuals.

Assume that the population habitats in an environment that is spatially heterogeneous yet continuous. As an initial attempt, we do not want to make things too complicated, and hence, we only consider the one dimensional full space $\mathbb{R} = (-\infty, \infty)$ as the spatial domain. The sub-populations in all four classes are thus tracked not only on time but also on location, leading to the notations $S = S(t, x)$, $L = L(t, x)$, $I = I(t, x)$, $R = R(t, x)$.

Since the disease has a latency and the latent individuals may move around, for any chosen location x, those infected in other locations may possibly have moved to this location when they have survived the latent period and entered the infectious class. In other words, the rate of change of infectious population at time t and location x depends on the new infections occurred in all other locations τ time units ago. In order to determine such a dependence, we introduce the infection age variable a. Denote by $E(t, a, x)$ the density (with respect to the infection age a) of the exposed population at time t and location x. A standard argument on population with age structure and spatial diffusion (see, e.g., Metz and Diekmann, 1986) gives

$$\frac{\partial E(t,a,x)}{\partial t} + \frac{\partial E(t,a,x)}{\partial a} = D(a)\frac{\partial^2 E(t,a,x)}{\partial x^2} - \big(\sigma(a) + \gamma(a) + d\big)E(t,a,x), \quad (1)$$

where $D(a)$, $\sigma(a)$ and $\gamma(a)$ are the diffusion rate, the disease-induced mortality rate and the recovery rate at age a, respectively, and d is the natural death rate which is independent on the infection age. Since the spatial domain $\mathbb{R}$ is the whole space, we need to propose the following boundary condition:

$$E(t, a, \pm\infty) < \infty. \quad (2)$$

By the meanings of τ and the density, it is obvious that

$$I(t,x) = \int_{\tau}^{\infty} E(t,a,x)\,da, \quad (3)$$

and

$$L(t,x) = \int_{0}^{\tau} E(t,a,x)\,da. \quad (4)$$

Here, ∞ can be replaced by a finite number larger than τ, say T, but this is just a matter of notation and causes no difference. Differentiating (3) with respect to t leads to

$$\begin{aligned}\frac{\partial I(t,x)}{\partial t} &= \int_\tau^\infty \frac{\partial}{\partial t}E(t,a,x)\,da \\ &= \int_\tau^\infty \Bigg(-\frac{\partial E(t,a,x)}{\partial a} + D(a)\frac{\partial^2 E(t,a,x)}{\partial x^2} \\ &\quad - \big(\sigma(a)+\gamma(a)+d\big)E(t,a,x)\Bigg)\,da \\ &= -\int_\tau^\infty \frac{\partial E(t,a,x)}{\partial a}\,da \\ &\quad + \int_\tau^\infty \Bigg(D(a)\frac{\partial^2 E(t,a,x)}{\partial x^2} - \big(\sigma(a)+\gamma(a)+d\big)E(t,a,x)\Bigg)\,da \\ &= -E(t,\infty,x) + E(t,\tau,x) \\ &\quad + \int_\tau^\infty \Bigg(D(a)\frac{\partial^2 E(t,a,x)}{\partial x^2} - \big(\sigma(a)+\gamma(a)+d\big)E(t,a,x)\Bigg)\,da \\ &= E(t,\tau,x) \\ &\quad + \int_\tau^\infty \Bigg(D(a)\frac{\partial^2 E(t,a,x)}{\partial x^2} - \big(\sigma(a)+\gamma(a)+d\big)E(t,a,x)\Bigg)\,da,\end{aligned}$$

where we have used the biologically realistic condition:

$$E(t,\infty,x) = 0.$$

Similarly, from (4), we can obtain

$$\begin{aligned}\frac{\partial L(t,x)}{\partial t} &= \int_0^\tau \frac{\partial E(t,a,x)}{\partial t}\,da \\ &= \int_0^\tau \Bigg(-\frac{\partial E(t,a,x)}{\partial a} + D(a)\frac{\partial^2 E(t,a,x)}{\partial x^2} \\ &\quad - \big(\sigma(a)+\gamma(a)+d\big)E(t,a,x)\Bigg)\,da \\ &= E(t,0,x) - E(t,\tau,x) \\ &\quad + \int_0^\tau \Bigg(D(a)\frac{\partial^2 E(t,a,x)}{\partial x^2} - \big(\sigma(a)+\gamma(a)+d\big)E(t,a,x)\Bigg)\,da.\end{aligned}$$

In order to proceed further, we make the following assumptions on those rate functions to simplify the model to some extent:

$$D(a) = D_I, \quad \sigma(a) = \sigma, \quad \gamma(a) = \gamma, \quad \text{for } a \in [\tau,\infty). \tag{5}$$

Also, notice that the new infections are due to the contact of infectious and susceptible individuals. We adopt the mass action infection mechanism that the lost of susceptible individuals by infection is at a rate proportional to the number of infectious and susceptible

individuals that is rSI, where $r > 0$ is a constant called infection rate, resulting in the following condition:

$$E(t, 0, x) = rI(t, x)S(t, x). \tag{6}$$

We further assume that in the absence of disease, the population would settle in a uniform steady state. One simple way to achieve this is to adopt the following simplest demographic equation for a population $N(t, x)$:

$$\frac{\partial N(t,x)}{\partial t} = \mu + D\frac{\partial^2 N(t,x)}{\partial x^2} - dN(t, x), \tag{7}$$

where $\mu > 0$ is a constant recruiting rate, D is the diffusion rate and d is the natural death rate. By the standard theory for partial differential equations on $\mathbb{R}$, one can easily see that every solution of (7) with a continuous and bounded initial function converges to the uniformly steady state $N = \mu/d$. We also assume that the disease under consideration does not transmit vertically. With these assumptions, the disease dynamics can be described by the following equations:

$$\begin{cases} \dfrac{\partial S(t,x)}{\partial t} = \mu + D_S\dfrac{\partial^2 S(t,x)}{\partial x^2} - dS(t, x) - rI(t, x)S(t, x), \\ \dfrac{\partial L(t,x)}{\partial t} = \displaystyle\int_0^\tau \left(D(a)\frac{\partial^2 E(t,a,x)}{\partial x^2} - \big(\sigma(a) + \gamma(a) + d\big)E(t, a, x)\right) da \\ \qquad\qquad + rI(t, x)S(t, x) - E(t, \tau, x), \\ \dfrac{\partial I(t,x)}{\partial t} = D_I\dfrac{\partial^2 I(t,x)}{\partial x^2} - (\sigma + \gamma + d)I(t, x) + E(t, \tau, x), \\ \dfrac{\partial R(t,x)}{\partial t} = D_R\dfrac{\partial^2 R(t,x)}{\partial x^2} + \displaystyle\int_0^\tau \gamma(a)E(t, a, x)\, da + \gamma I(t, x) - dR(t, x). \end{cases} \tag{8}$$

Here, μ is now explained as the recruitment of the susceptible individuals, and D_S and D_R are constants representing the spatial diffusion rates of susceptible and removed individuals, respectively.

Note that in (8), $S(t, x)$ is decoupled from $L(t, x)$ and $R(t, x)$, but $I(t, x)$ is seemingly affected by $L(t, x)$ through $E(t, \tau, x)$. If we can determine $E(t, \tau, x)$ in terms of S and I, then the resulting S and I equations form an independent system that can be used as a model to describe the disease dynamics. By the meaning of $E(t, \tau, x)$, it indeed gives the rate at which location x gains the individuals who are just entering the infectious stage.

For fix $s \geq 0$, let

$$V^s(t, x) = E(t, t - s, x), \quad \text{for } s \leq t \leq s + \tau. \tag{9}$$

By (1), we then have

$$\begin{aligned} \frac{\partial}{\partial t}V^s(t, x) &= \frac{\partial}{\partial t}E(t, a, x)|_{a=t-s} + \frac{\partial}{\partial a}E(t, a, x)|_{a=t-s} \\ &= D(t - s)\frac{\partial^2}{\partial x^2}V^s(t, x) - \big(\sigma(t - s) + \gamma(t - s) + d\big)V^s(t, x). \end{aligned} \tag{10}$$

This is a linear reaction-diffusion equation for $V^s(t,x)$ and can be solved explicitly according to the corresponding boundary conditions. The boundary condition (2) directly translates to

$$\left|V^s(t,\pm\infty)\right| < \infty. \tag{11}$$

Applying the method of separation of variables to (10)–(11), we obtain

$$\begin{aligned} V^s(t,x) &= \int_{-\infty}^{\infty} k(s,\omega) \\ &\quad \times \exp\left(-\int_s^t \left(\omega^2 D(\theta-s)+\sigma(\theta-s)+\gamma(\theta-s)+d\right)d\theta\right)e^{-i\omega x}\,d\omega \\ &= \int_{-\infty}^{\infty} k(s,\omega)\exp\left(-\int_0^{t-s}\left(\omega^2 D(a)+\sigma(a)+\gamma(a)+d\right)da\right)e^{-i\omega x}\,d\omega. \end{aligned} \tag{12}$$

By (6) and (9), we notice that

$$rI(s,x)S(s,x) = E(s,0,x) = V^s(s,x) = \int_{-\infty}^{\infty} k(s,\omega)e^{-i\omega x}\,d\omega.$$

That is, $rI(s,x)S(s,x)$ is the Fourier transform of $k(s,\omega)$. Therefore, $k(s,\omega)$ is the inverse Fourier transform of $rI(s,x)S(s,x)$, and hence

$$k(s,\omega) = \frac{1}{2\pi}\int_{-\infty}^{\infty} rI(s,y)S(s,y)e^{i\omega y}\,dy. \tag{13}$$

For the infection age $a\in[0,\tau]$, we distinctly denote by $D_L(a)$, $\sigma_L(a)$, and $\gamma_L(a)$ the diffusion rate, the disease mortality rate, and the recovery rate, respectively. For simplicity, we assume that these rates are all constants, that is,

$$\begin{aligned} &D(a) = D_L(a) = D_L, \quad \sigma(a) = \sigma_L(a) = \sigma_L, \\ &\gamma(a) = \gamma_L(a) = \gamma_L, \quad \text{for } a\in[0,\tau]. \end{aligned} \tag{14}$$

Let

$$\bar{d} := \sigma_L + \gamma_L + d, \qquad \alpha := \int_0^{\tau} D(a)\,da = \tau D_L, \quad \text{and} \quad \epsilon := e^{-\bar{d}\tau}. \tag{15}$$

Obviously, α is a measurement of the mobility of the latent individuals and ϵ measures the proportion of the infected individuals that can survive the latent period. Now by (9)–(13), we can determine $E(t,\tau,x)$ as below:

$$\begin{aligned} E(t,\tau,x) &= V^{t-\tau}(t,x) \\ &= \int_{-\infty}^{\infty} k(t-\tau,\omega)\exp\left(-\int_0^{t-(t-\tau)}\left(\omega^2 D_L(a)+\bar{d}\right)da\right)e^{-i\omega x}\,d\omega \end{aligned}$$

$$
\begin{aligned}
&= \int_{-\infty}^{\infty} \frac{1}{2\pi} \int_{-\infty}^{\infty} rI(t-\tau, y)S(t-\tau, y)e^{i\omega y}\, dy \\
&\quad \times \exp\left(-\int_0^{\tau} \left(\omega^2 D_L(a) + \bar{d}\right) da\right) e^{-i\omega x}\, d\omega \\
&= \frac{1}{2\pi} \int_{-\infty}^{\infty} \int_{-\infty}^{\infty} rI(t-\tau, y)S(t-\tau, y)e^{i\omega(y-x)} \\
&\quad \times \exp\left(-\int_0^{\tau} \left(\omega^2 D_L(a) + \bar{d}\right) da\right) dy\, d\omega \\
&= \frac{1}{2\pi} \int_{-\infty}^{\infty} rI(t-\tau, y)S(t-\tau, y) \\
&\quad \times \exp\left(-\int_0^{\tau} \bar{d}\, da\right) \left(\int_{-\infty}^{\infty} e^{-\alpha\omega^2} e^{i\omega(y-x)}\, d\omega\right) dy \\
&= \frac{1}{2\pi} \int_{-\infty}^{\infty} rI(t-\tau, y)S(t-\tau, y)e^{-\bar{d}\tau} \sqrt{\frac{\pi}{\alpha}} e^{-\frac{(x-y)^2}{4\alpha}}\, dy \\
&= \frac{\epsilon}{\sqrt{4\pi\alpha}} \int_{-\infty}^{\infty} rI(t-\tau, y)S(t-\tau, y)e^{-\frac{(x-y)^2}{4\alpha}}\, dy. \qquad (16)
\end{aligned}
$$

Here, we have used the fact that the Fourier transform of the function $\sqrt{\pi/\alpha}e^{-x^2/4\alpha}$ is $e^{-\alpha w^2}$. Plugging (16) into the I equation in (8) results in

$$
\begin{aligned}
\frac{\partial I(t,x)}{\partial t} &= D_I \frac{\partial^2 I(t,x)}{\partial x^2} - (\sigma + \gamma + d)I(t,x) \\
&\quad + \epsilon \int_{-\infty}^{\infty} rI(t-\tau, y)S(t-\tau, y) f_\alpha(x-y)\, dy, \qquad (17)
\end{aligned}
$$

where

$$
f_\alpha(x) = \frac{1}{\sqrt{4\pi\alpha}} e^{-\frac{x^2}{4\alpha}}.
$$

By (14), (15), and (16), the L equation in (8) becomes

$$
\begin{aligned}
\frac{\partial L(t,x)}{\partial t} &= D_L \frac{\partial^2 L(t,x)}{\partial x^2} + rI(t,x)S(t,x) - \bar{d}L(t,x) \\
&\quad - \epsilon \int_{-\infty}^{\infty} rI(t-\tau, y)S(t-\tau, y) f_\alpha(x-y)\, dy. \qquad (18)
\end{aligned}
$$

Therefore, the full model (8) reduces to

$$\begin{cases} \dfrac{\partial S(t,x)}{\partial t} = \mu + D_S \dfrac{\partial^2 S(t,x)}{\partial x^2} - dS(t,x) - rI(t,x)S(t,x), \\ \dfrac{\partial L(t,x)}{\partial t} = D_L \dfrac{\partial^2 L(t,x)}{\partial x^2} + rI(t,x)S(t,x) - \bar{d}L(t,x) \\ \qquad\qquad - \epsilon \displaystyle\int_{-\infty}^{\infty} rI(t-\tau,y)S(t-\tau,y) f_\alpha(x-y)\,dy, \\ \dfrac{\partial I(t,x)}{\partial t} = D_I \dfrac{\partial^2 I(t,x)}{\partial x^2} - (\sigma+\gamma+d)I(t,x) \\ \qquad\qquad + \epsilon \displaystyle\int_{-\infty}^{\infty} rI(t-\tau,y)S(t-\tau,y) f_\alpha(x-y)\,dy, \\ \dfrac{\partial R(t,x)}{\partial t} = D_R \dfrac{\partial^2 R(t,x)}{\partial t} + \gamma_L L(t,x) + \gamma I(t,x) - dR(t,x). \end{cases} \tag{19}$$

From (19), we see that the equations for $S(t,x)$ and $I(t,x)$ are fully decoupled from the equations for $L(x,t)$ and $R(t,x)$. Hence, we only need to consider S and I equations which form the following sub-system:

$$\begin{cases} \dfrac{\partial S(t,x)}{\partial t} = \mu + D_S \dfrac{\partial^2 S(t,x)}{\partial x^2} - dS(t,x) - rI(t,x)S(t,x), \\ \dfrac{\partial I(t,x)}{\partial t} = D_I \dfrac{\partial^2 I(t,x)}{\partial x^2} - \beta I(t,x) \\ \qquad\qquad + \epsilon \displaystyle\int_{-\infty}^{\infty} rI(t-\tau,y)S(t-\tau,y) f_\alpha(x-y)\,dy, \end{cases} \tag{20}$$

for $t > 0$ and $x \in \mathbb{R}$, where we have introduced $\beta = \sigma + \gamma + d$. Biologically, we are more concerned about the population sizes of susceptible and infectious individuals in the whole population.

To conclude this section, we remark that it may not be realistic to assume non-zero recovery rate and disease induced death rate in the latent period. However, these rates may become non-zero in later stages, and our goal is to set up a general framework that is applicable to as wide a range of diseases as possible. On the other hand, including these two rates in every stage in the model does not cause extra difficulty since they are all absorbed into the parameter $\bar{d}$ and β. Thus, for consideration of generality, we decide to include these two rates in all stages. In our numeric simulations, these two rates in latent stage are all taken to be zero. For the same consideration of generality, we start in the (1) with general diffusion rate D depending on the infection age. In reality, there are diseases for which the infectious individual become less mobile (e.g., influenza); there are also diseases for which the infectious individuals actually become more mobile (e.g., rabies). Of course, there are also diseases for which the mobility remains almost the same for individuals in all stages. This reality justifies the need of considering structured diffusion rate which, of course, increases the difficulty level in analyzing the model. After adopting less general assumption that the diffusion rate is constant in each stage of infection, the model has reduced to (20), with which we will deal in the rest of this paper.

3. Existence, uniqueness and positivity of solutions of the Cauchy problem

Model (20) is a delayed reaction-diffusion system with a non-local reaction term on the whole spatial domain $\mathbb{R} = (-\infty, \infty)$. Naturally, an initial condition of the delayed type is needed for (20), as is for any other delay differential equation models. In other words, we need to consider the following initial value problem

$$\begin{cases} \dfrac{\partial S(t,x)}{\partial t} = \mu + D_S \Delta S(t,x) - dS(t,x) - rI(t,x)S(t,x), \quad x \in \mathbb{R},\ t > 0, \\ \dfrac{\partial I(t,x)}{\partial t} = D_I \Delta I(t,x) - \beta I(t,x) \\ \qquad\qquad + \epsilon \displaystyle\int_{-\infty}^{\infty} rI(t-\tau, y)S(t-\tau, y) f_\alpha(x-y)\, dy, \quad x \in \mathbb{R},\ t > 0, \\ S(\theta, x) = \phi_S(\theta, x) \quad \text{and} \quad I(\theta, x) = \phi_I(\theta, x), \quad \text{for } x \in \mathbb{R},\ \theta \in [-\tau, 0], \end{cases} \tag{21}$$

where Δ is the Laplacian operator on $\mathbb{R}$, and ϕ_S and ϕ_I are the initial functions which will be specified below.

For convenience of proceeding, denote by $X = \mathrm{BUC}(\mathbb{R}, \mathbb{R}^2)$ the set of all bounded and uniformly continuous functions from $\mathbb{R}$ to $\mathbb{R}^2$. With the usual supremum norm, X is a Banach space. Let

$$X^+ := \big\{ \boldsymbol{\Phi} \in X : \boldsymbol{\Phi}(x) \geq \mathbf{0},\ \text{for all } x \in \mathbb{R} \big\}.$$

It is easy to see that X^+ is a closed cone of X and X is a Banach lattice under the partial ordering induced by X^+. Let $\mathbf{D} := [D_S, D_I]^T$ with T representing the transpose of matrices and vectors. From Theorem 1.5 in Daners and Medina (1992), it follows that the X-realization $\mathbf{D}\Delta_X$ of $\mathbf{D}\Delta$ generates an analytic semi-group $\mathbf{T}(t)$ on X.

Denote $\mathbf{U}(t,x) = [S(t,x), I(t,x)]^T$ and $\boldsymbol{\Phi}(x) = [\phi_S(x), \phi_I(x)]^T$. It is known that the solution of the initial value problem

$$\begin{cases} \dfrac{\partial \mathbf{U}(t,x)}{\partial t} = \mathbf{D}\Delta \mathbf{U}(t,x), \quad x \in \mathbb{R},\ t > 0, \\ \mathbf{U}(0,x) = \boldsymbol{\Phi}(x), \quad x \in \mathbb{R}, \end{cases} \tag{22}$$

can be expressed in terms of the heat kernel as the following:

$$\mathbf{U}(t,x) = \big(\mathbf{T}(t)\boldsymbol{\Phi}\big)(x) = \begin{bmatrix} \dfrac{1}{\sqrt{4\pi D_S t}} \displaystyle\int_{-\infty}^{\infty} \exp\left(-\frac{(x-y)^2}{4D_S t}\right)\phi_S(y)\, dy \\ \dfrac{1}{\sqrt{4\pi D_I t}} \displaystyle\int_{-\infty}^{\infty} \exp\left(-\frac{(x-y)^2}{4D_I t}\right)\phi_I(y)\, dy \end{bmatrix},$$
$$x \in \mathbb{R},\ t > 0,\ \boldsymbol{\Phi} \in X. \tag{23}$$

It follows immediately from (23) that

$$\mathbf{T}(t)X^+ \subset X^+.$$

Let $C = C([-\tau, 0], X)$ be the Banach space of continuous functions from $[-\tau, 0]$ to X with the supremum norm $\|\cdot\|$ and let

$$C^+ = \{\mathbf{\Phi} \in C : \mathbf{\Phi}(s) \in X^+, \text{ for all } s \in [-\tau, 0]\}.$$

Then C^+ is a closed cone of C. For convenience, we identify an element $\mathbf{\Phi} \in C$ as a function from $[-\tau, 0] \times \mathbb{R}$ into $\mathbb{R}^2$ by $\mathbf{\Phi}(s, x) = \mathbf{\Phi}(s)(x)$. For any continuous function $y(\cdot) : [-\tau, b) \to X$, where $b > 0$, we define $y_t \in C$, $t \in [0, b)$, by $y_t(s) = y(t + s)$, $s \in [-\tau, 0]$. It is well known that $t \mapsto y_t$ is a continuous function from $[0, b)$ to C. The right-hand side of (21) induces a non-linear functional $\mathbf{F} : C^+ \to X$ by

$$\mathbf{F}(\mathbf{\Phi})(x) = \begin{bmatrix} \mu - d\phi_S(0, x) - r\phi_S(0, x)\phi_I(0, x) \\ -\beta\phi_I(0, x) + \epsilon \int_{-\infty}^{\infty} r\phi_S(-\tau, x)\phi_I(-\tau, x) f_\alpha(x - y)\, dy \end{bmatrix},$$

$$x \in \mathbb{R}, \mathbf{\Phi} \in C^+.$$

Moreover, we know that the restriction of the product function $g(x, y) = xy$ to $[0, \infty) \times [0, \infty)$ is positive and locally Lipschitz continuous, thus

$$\lim_{h \to 0} d\big(\mathbf{\Phi}(0) + h\mathbf{F}(\mathbf{\Phi}), X^+\big) := \lim_{h \to 0} \inf\big\{\big|\mathbf{\Phi}(0) + h\mathbf{F}(\mathbf{\Phi}) - \xi\big|_X : \xi \in X^+\big\} = 0,$$

$$\text{for } \mathbf{\Phi} \in C^+,$$

and for any $R > 0$, there exists $L_R > 0$ such that

$$\big|\mathbf{F}(\mathbf{\Phi}) - \mathbf{F}(\mathbf{\Psi})\big|_X \le L_R \|\mathbf{\Phi} - \mathbf{\Psi}\|, \quad \text{if } \mathbf{\Phi}, \mathbf{\Psi} \in C^+, \text{and } \|\mathbf{\Phi}\|, \|\mathbf{\Psi}\| \le R.$$

Consequently, from Martin Jr and Smith (1990) (or Corollary 1.3 on p. 270 of Wu, 1996), we know that for each $\mathbf{\Phi} \in C^+$ there exists a unique non-continuable solution $\mathbf{W}$ on $[0, t_{\mathbf{\Phi}})$, for some $t_{\mathbf{\Phi}} > 0$, of the following initial-value problem for the abstract integral equation:

$$\begin{cases} \mathbf{W} = \mathbf{T}(t)\mathbf{W}(0) + \int_0^t \mathbf{T}(t - s)\mathbf{F}(\mathbf{W}_s)\, ds, \\ \mathbf{W}_0 = \mathbf{\Phi} \in C^+, \end{cases} \tag{24}$$

which satisfies $\mathbf{W}(t) \in X^+$ for all $t \in [0, t_{\mathbf{\Phi}})$. This solution is called the mild solution of (21). Since the semi-group $\mathbf{T}(t)$ is analytic, the mild solution of (21) must also be a classical solution of (21) for $t > \tau$ (see Corollary 2.5 on p. 50 in Wu, 1996). Therefore, we have proved that if the initial functions $\phi_S(\theta, x)$ and $\phi_I(\theta, x)$ in (21) are bounded, uniformly continuous, and non-negative, then (21) has a unique solution which is non-negative.

4. Traveling wave solution of (20)

In this section, we investigate the traveling wave solution of (20) which may arise due to the diffusion effect as well as the interaction between susceptible and infectious individuals. A traveling wave solution of (20) is a special solution of the form $S(t, x) = \phi(x + ct)$

and $I(t,x)=\psi(x+ct)$, with $c>0$ being the wave speed. If (20) has two constant steady states $\mathbf{U}_-=(S_-,I_-)$ and $\mathbf{U}_+=(S_+,I_+)$ such that the profile functions ϕ and ψ satisfy $\phi(-\infty)=S_-$, $\psi(-\infty)=I_-$, $\phi(+\infty)=S_+$ and $\psi(+\infty)=I_+$, then the traveling wave solution is called a traveling wave front connecting the two equilibria $\mathbf{U}_-$ and $\mathbf{U}_+$. Biologically, a traveling wave front connecting $\mathbf{U}_-$ and $\mathbf{U}_+$ accounts for the transition from equilibrium $\mathbf{U}_-$ to equilibrium $\mathbf{U}_+$ as time goes, and the wave speed may explain the spatial spread speed of the disease, and thus may measure how fast the disease invades geographically. Therefore, the traveling wave front is a very important topic for disease models with spatial heterogeneity.

We first identify possible constant steady states (also called equilibria). It is easily seen that $(S^0,I^0)=(\mu/d,0)$ is the disease free equilibrium for (20). Furthermore, under the additional assumption that

$$\mu\epsilon r-\beta d>0, \tag{25}$$

the model (20) has one and only one endemic equilibrium given by $(S^*,I^*)=(\beta/r\epsilon,\mu\epsilon/\beta-d/r)$.

As we mentioned above, a biologically and mathematically interesting and important problem is the existence of a traveling wave solution connecting (S^0,I^0) and (S^*,I^*). Substituting

$$S(t,x)=\phi(z),\quad I(t,x)=\psi(z),\quad z=x+ct,$$

into (20) gives the following system of delayed ordinary differential equations

$$\begin{cases} c\phi'(z)=\mu+D_S\phi''(z)-d\phi(z)-r\phi(z)\psi(z),\\ c\psi'(z)=D_I\psi''(z)-\beta\psi(z)\\ \qquad\qquad +\epsilon\displaystyle\int_{-\infty}^{+\infty} r\phi(z-y-c\tau)\psi(z-y-c\tau)f_\alpha(y)\,dy, \end{cases} \tag{26}$$

where the prime denotes differentiation with respect to z. We need to determine values of $c>0$ for which the DDE system (26) has a positive solution satisfying the following so-called asymptotic boundary conditions:

$$\phi(-\infty)=\frac{\mu}{d},\qquad \phi(+\infty)=\frac{\beta}{r\epsilon}\quad\text{and}\quad \psi(-\infty)=0,\qquad \psi(+\infty)=\frac{\mu\epsilon}{\beta}-\frac{d}{r}. \tag{27}$$

Thus, this is essentially an eigenvalue problem. Note that the second equation in (26) contains a non-local term in the form of integral over $\mathbb{R}$, this is indeed a non-trivial (actually very hard) problem.

To proceed further, we linearize (26) at $(S^0,I^0)=(\mu/d,0)$ to obtain some information about solutions of (26) near (S^0,I^0). The linearization is

$$\begin{cases} c\bar\phi'(z)=D_S\bar\phi''(z)-d\bar\phi(z)-\dfrac{r\mu}{d}\bar\psi(z),\\ c\bar\psi'(z)=D_I\bar\psi''(z)-\beta\bar\psi(z)+\dfrac{\epsilon r\mu}{d}\displaystyle\int_{-\infty}^{+\infty}\bar\psi(z-y-c\tau)f_\alpha(y)\,dy. \end{cases} \tag{28}$$

Plugging the trial functions $[\bar{\phi}(z), \bar{\psi}(z)]^T = [K_1 e^{\lambda z}, K_2 e^{\lambda z}]^T$ into (28), where $[K_1, K_2]$ is an arbitrary non-trivial constant vector, we obtain the characteristic equation for the linearization (28) as follows:

$$\left(D_S\lambda^2 - c\lambda - d\right)\left(D_I\lambda^2 - c\lambda - \beta + \frac{\epsilon r\mu}{d}\int_{-\infty}^{+\infty} e^{-\lambda(y+c\tau)} f_\alpha(y)\,dy\right) = 0. \tag{29}$$

Let

$$\Lambda_1(\lambda) \triangleq D_S\lambda^2 - c\lambda - d,$$
$$\Lambda_2(\lambda) \triangleq D_I\lambda^2 - c\lambda - \beta + \frac{\epsilon r\mu}{d}\int_{-\infty}^{+\infty} e^{-\lambda(y+c\tau)} f_\alpha(y)\,dy.$$

The equation $\Lambda_1(\lambda) = 0$ always have two real roots given by

$$\lambda_1 = \frac{c - \sqrt{c^2 + 4D_S d}}{2D_S} < 0, \qquad \lambda_2 = \frac{c + \sqrt{c^2 + 4D_S d}}{2D_S} > 0.$$

Analysis of the roots of $\Lambda_2(\lambda) = 0$ is much complicated. Firstly, noting that $\alpha = \tau D_L$ and

$$\begin{aligned}\int_{-\infty}^{+\infty} e^{-\lambda(y+c\tau)} f_\alpha(y)\,dy &= \frac{1}{\sqrt{4\pi\alpha}}\int_{-\infty}^{+\infty} e^{-\lambda(y+c\tau)} e^{-\frac{y^2}{4\alpha}}\,dy \\ &= \frac{1}{\sqrt{4\pi\alpha}}\int_{-\infty}^{+\infty} e^{-\frac{1}{4\alpha}(y+2\alpha\lambda)^2}dy\, e^{\alpha\lambda^2 - \lambda c\tau} \\ &= e^{\alpha\lambda^2 - \lambda c\tau},\end{aligned}$$

the equation $\Lambda_2(\lambda) = 0$ can be rewritten as

$$\frac{\epsilon r\mu}{d} e^{\tau D_L\lambda^2 - \lambda c\tau} = -D_I\lambda^2 + c\lambda + \beta. \tag{30}$$

Let

$$g(\lambda, c) = \frac{\epsilon r\mu}{d} e^{\tau D_L\lambda^2 - \lambda c\tau} \quad \text{and} \quad h(\lambda, c) = -D_I\lambda^2 + c\lambda + \beta. \tag{31}$$

By fundamental calculus, it is easy to see that there is a $c^* > 0$ such that when $c < c^*$, all roots of (30) are complex; when $c > c^*$, (30) will have two real positive roots. Indeed, c^* is determined by the original Eq. (30) and an extra tangent condition:

$$g(\lambda, c) = h(\lambda, c) \quad \text{and} \quad g'_\lambda(\lambda, c) = h'_\lambda(\lambda, c). \tag{32}$$

See Figs. 1, 2, and 3 for a demonstration for the case $D_I = D_L$. Therefore, for $c < c^*$, (26) can not have a *positive* solution satisfying (27), because a solution of (26) near $(\mu/d, 0)$ oscillates about $(\mu/d, 0)$, and thus the ψ component of the solution of (26) will take *negative* values.

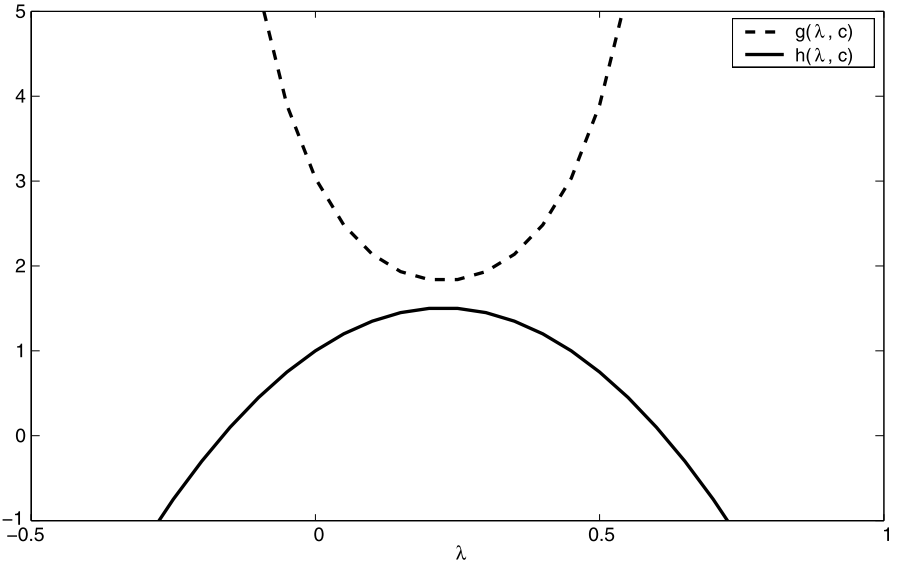

Fig. 1 $\min_\lambda g(\lambda, c) > \max_\lambda h(\lambda, c)$ with parameters values: $\mu = 5$, $d = 0.5$, $r = 0.5$, $\sigma_L = \gamma_L = 0$, $\sigma = 0.25$, $\gamma = 0.25$, $\tau = 1$, $D_S = D_L = D_I = 10$, $c = 4.5$. For these parameter values, $c^* = 4.9974$.

More information about c^* is helpful but not easy to obtain in general. In the sequel, we focus on a special situation when $D_L = D_I$. In such a case, for any $c > 0$, both $m(c) \triangleq \min_\lambda g(\lambda, c)$ and $M(c) \triangleq \max_\lambda h(\lambda, c)$ are attained at the same value of λ: $\lambda = \frac{c}{2D_I}$, giving

$$m(c) = \min_\lambda g(\lambda, c) = g\left(\frac{c}{2D_L}, c\right) = \frac{\epsilon r \mu}{d} e^{-\frac{c^2\tau}{4D_L}} = \frac{\epsilon r \mu}{d} e^{-\frac{c^2\tau}{4D_I}},$$

and

$$M(c) = \max_\lambda h(\lambda, c) = h\left(\frac{c}{2D_I}, c\right) = \frac{c^2}{4D_I} + \beta.$$

Therefore, (30) has real roots if and only if

$$m(c) < M(c) \quad \text{i.e. } \frac{\epsilon r \mu}{d} e^{-\frac{c^2\tau}{4D_L}} < \frac{c^2}{4D_I} + \beta. \tag{33}$$

Denote by z^* the unique positive solution of

$$\frac{\epsilon r \mu}{d} e^{-\tau z} = z + \beta, \tag{34}$$

under the condition (25) (see Fig. 4). It follows from (33) and the preceding discussion that c^* can be obtained by solving $\frac{c^2}{4D_I} = z^*$, that is,

$$c^* = 2\sqrt{D_I z^*}. \tag{35}$$

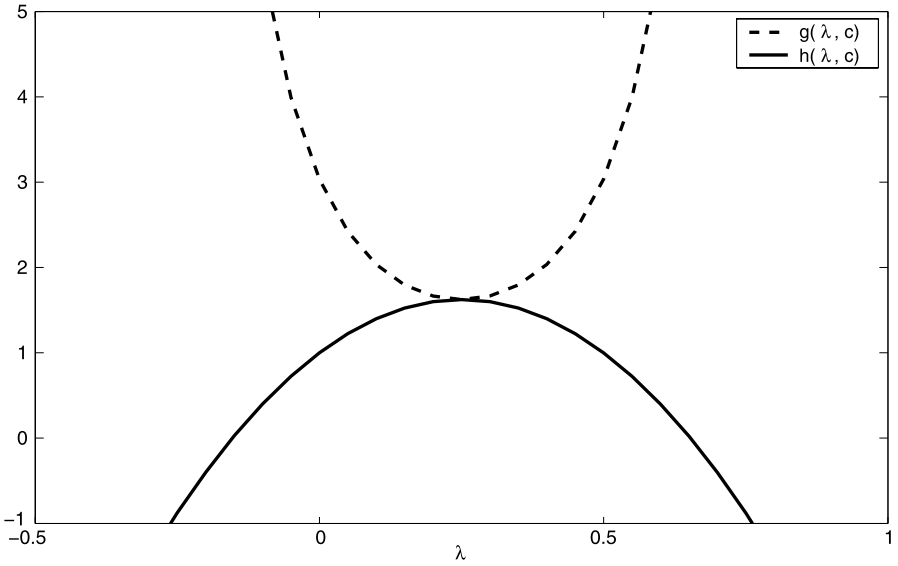

Fig. 2 $\min_\lambda g(\lambda, c) = \max_\lambda h(\lambda, c)$ with parameters values: $\mu = 5$, $d = 0.5$, $r = 0.5$, $\sigma_L = \gamma_L = 0$, $\sigma = 0.25$, $\gamma = 0.25$, $\tau = 1$, $D_S = D_L = D_I = 10$, $c = 4.9974 = c^*$.

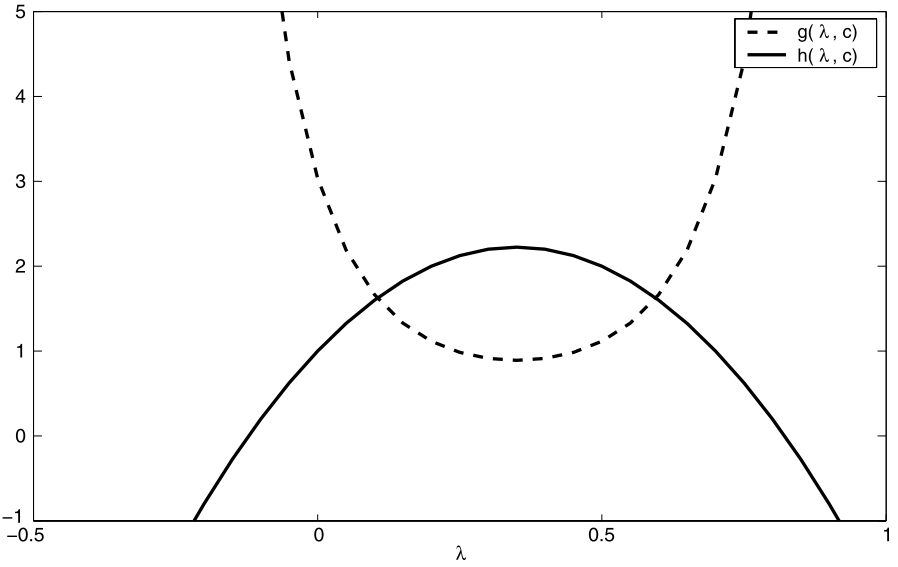

Fig. 3 $\min_\lambda g(\lambda, c) < \max_\lambda h(\lambda, c)$ with parameters values: $\mu = 5$, $d = 0.5$, $r = 0.5$, $\sigma_L = \gamma_L = 0$, $\sigma = 0.25$, $\gamma = 0.25$, $\tau = 1$, $D_S = D_L = D_I = 10$, $c = 6 > 4.9974 = c^*$.

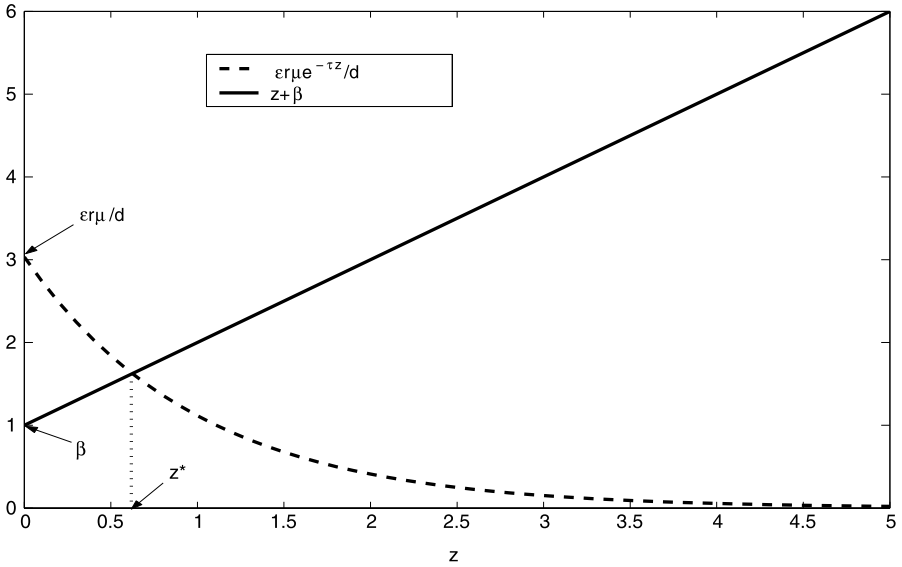

Fig. 4 How z^* is determined.

Notice that $z^* > 0$ depends on τ and is actually a decreasing function of τ, so is c^*. When $\tau = 0$, $z^* = r\mu/d - \beta$ and hence c^* can be explicitly given by $c^* = 2\sqrt{D_I(r\mu/d - \beta)}$.

Summarizing the above, we have obtained, under the condition (25), a lower bound c^* of speed for the traveling wave front connecting (S^0, I^0) and (S^*, I^*), in the sense that when $c < c^*$, traveling wave fronts with speed c connecting (S^0, I^0) and (S^*, I^*) are impossible. Unfortunately, in this project, we are unable to prove that c^* is the minimal wave speed in the sense that for every $c \geq c^*$, there is a traveling wave front connecting (S^0, I^0) and (S^*, I^*). This is mainly due to the prey-predator interaction nature of the model, as well as to the presence of both the latent delay τ and integral term arising from the non-local infection in (26). It is well known that the existence of traveling wave fronts in a diffusive prey-predator system has been a long time challenging mathematical problem and only very few results have been obtained but for local systems without time delay (see, e.g., Dunbar 1981, 1983, 1984; Gardner, 1984; Huang et al., 2003). In the next section, we will numerically investigate the existence of traveling wave fronts of (20) connecting (S^0, I^0) and (S^*, I^*). As we will see in Section 5, the simulation results seem to suggest that c^* is the minimal wave speed.

5. Numerical simulations

In this section, using the results obtained in Section 4 as guidelines, we perform some numeric simulations. We first numerically investigate the existence of positive solutions to the system (26) satisfying the asymptotic boundary condition (27), i.e. the traveling wave solutions of the system (20) that connect the disease free equilibrium and the endemic equilibrium. In addition, we will also simulate solutions of the original functional partial

differential system (20) to observe the evolution of solutions to the initial value problem toward a traveling wave front. Note that our model contains a time delay representing the latent period, as well as a non-local infection term due to the mobility of the individuals in the latent period, the simulations are non-trivial at all. The details of the numeric methods we use to perform the simulations are described in the Appendix. In this section, we only give the simulation results.

As in the demonstrating figures (Figs. 1, 2, and 3) in Section 4, the following parameter values are used here again:

$$\begin{aligned} &\mu = 5, \qquad d = 0.5, \qquad r = 0.5, \qquad \sigma_L = \gamma_L = 0, \\ &\sigma = 0.25, \qquad \gamma = 0.25, \qquad D_S = 10, \qquad D_L = D_I = 10. \end{aligned} \tag{36}$$

It is easily verified that (25) is satisfied for these values. Indeed, for these values, the disease free equilibrium is $(S^0, I^0) = (10, 0)$ and the endemic equilibrium is $(S^*, I^*) = (3.2974, 2.0327)$.

The above parameter values belong to the case when $D_L = D_I$, corresponding to which, c^* is determined by (34) and (35). We have seen in Section 4 that c^* depends on τ. For the above parameter values with $\tau = 1$, c^* is numerically computed as $c^* = 4.9974$.

Figure 5 is the simulation result for $c = 6 > 4.9974 = c^*$, clearly showing the existence of positive solution of (26) and (27), and thus supporting our conjecture in Section 4. Note that the profile of the traveling wave front is not monotone, this seems to be due to the feature of the prey-predator interaction. When c decreases to pass c^*, our analysis in Section 4 concludes positive solutions of (26) and (27) become impossible, because the ψ component of the solution will take some negative values. This conclusion is shown in Figs. 6, 7, 8 with the observation that the further below c^* the value of c is, the more obvious the oscillations of ψ about I^0 are.

Next, we give some simulation results for (20), using the method described in Appendix A.2. For this purpose, we truncate the spatial domain $\mathbb{R}$ by $[-200, 200]$. For convenience, we use the following piecewise functions as initial conditions:

$$S(t,x) = \begin{cases} S^*, & -200 \le x \le 0, \ -\tau \le t \le 0, \\ S^0, & 0 \le x \le 200, \ -\tau \le t \le 0, \end{cases}$$

and

$$I(t,x) = \begin{cases} I^*, & -200 \le x \le 0, \ -\tau \le t \le 0, \\ I^0, & 0 \le x \le 200, \ -\tau \le t \le 0. \end{cases}$$

For this part, the following parameter values will be fixed:

$$\begin{aligned} &\mu = 5, \qquad d = 0.5, \qquad r = 0.5, \\ &\sigma_L = \gamma_L = 0, \qquad \sigma = 0.25, \qquad \gamma = 0.25. \end{aligned} \tag{37}$$

We do not fix the diffusion rates since we want to observe the impact of these rates on the traveling wave speed c which does not appear in (20), but which we hope to be able to observe from the simulation results.

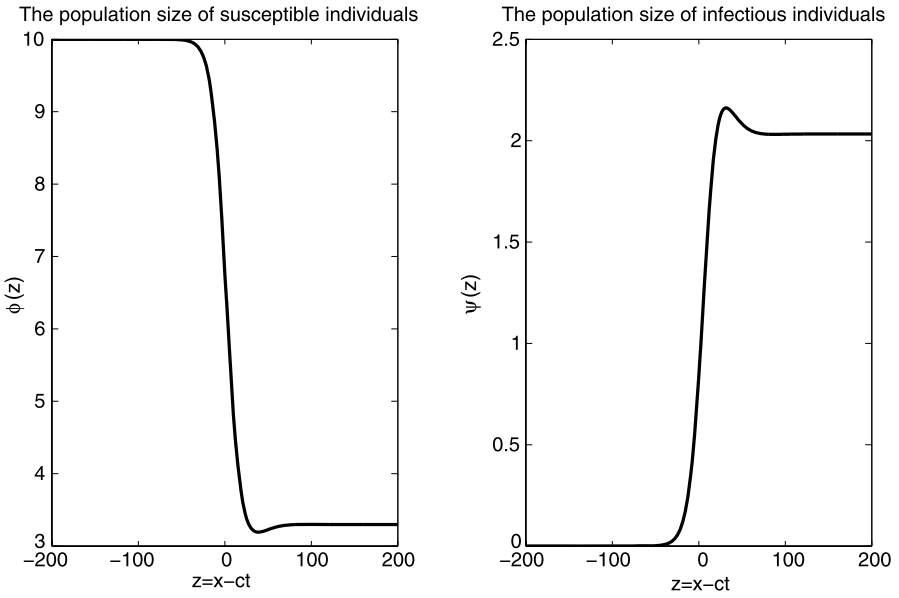

Fig. 5 Assuming (36) and with $\tau = 1$ and $c = 6 > c^* = 4.9974$, there is a traveling wave front with speed $c = 6$.

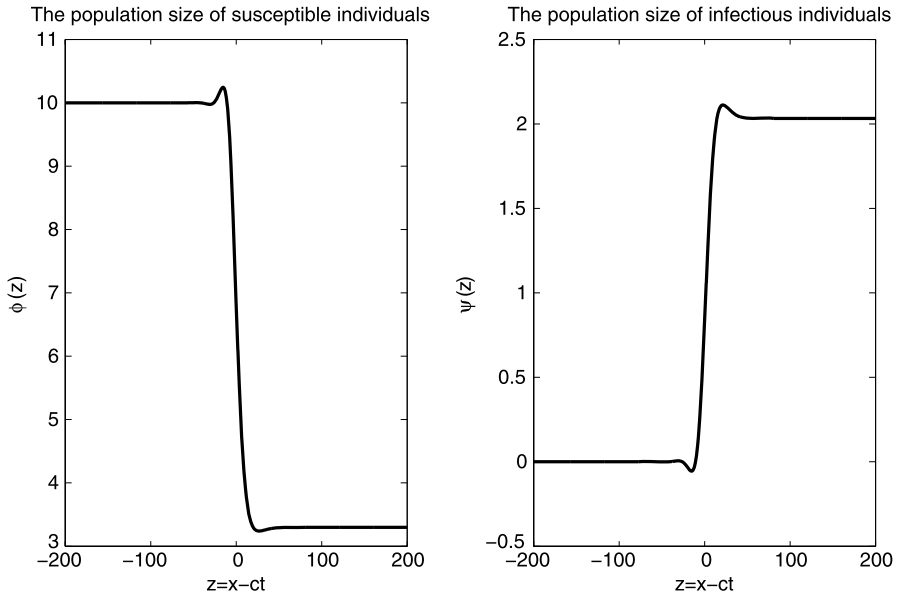

Fig. 6 Assuming (36) and with $\tau = 1$ and $c = 3 < c^* = 4.9974$, there is no traveling wave front with speed $c = 3$: ψ may take negative values.

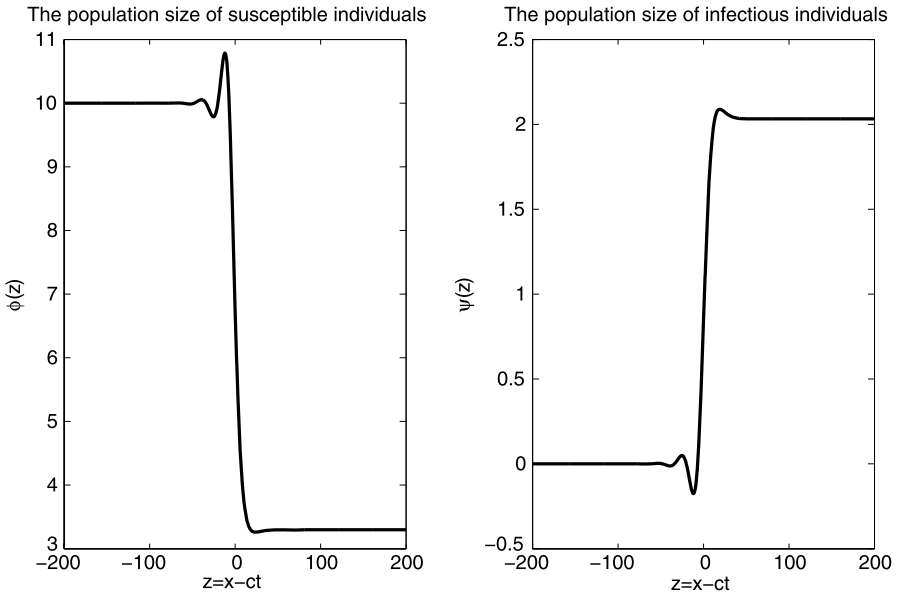

[p]

Fig. 7 Assuming (36) and with $\tau = 1$ and $c = 2 < c^* = 4.9974$, there is no traveling wave front with speed $c = 2$: ψ may take negative values.

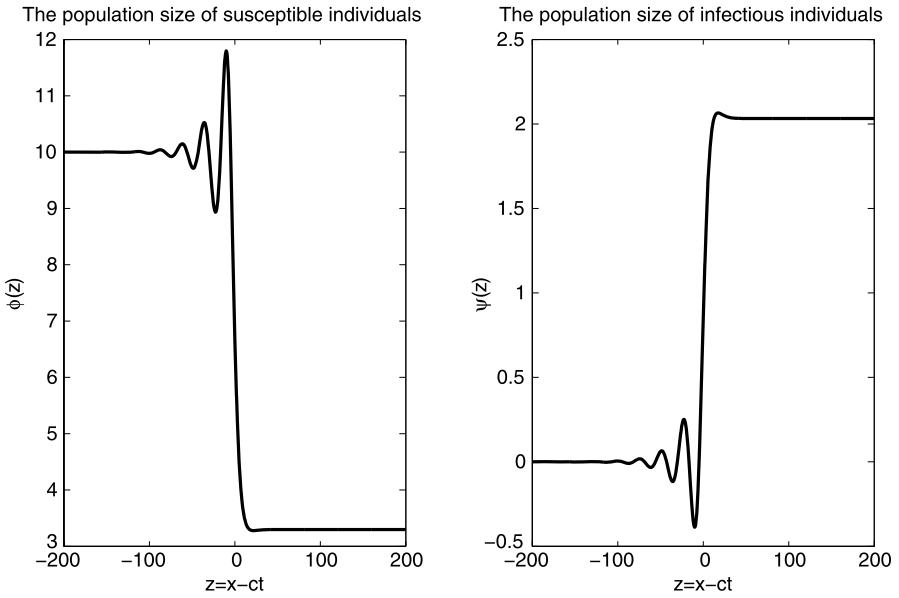

Fig. 8 Assuming (36) and with $\tau = 1$ and $c = 1 < c^* = 4.9974$, there is no traveling wave front with speed $c = 1$: ψ may take negative values and actually oscillates about 0.

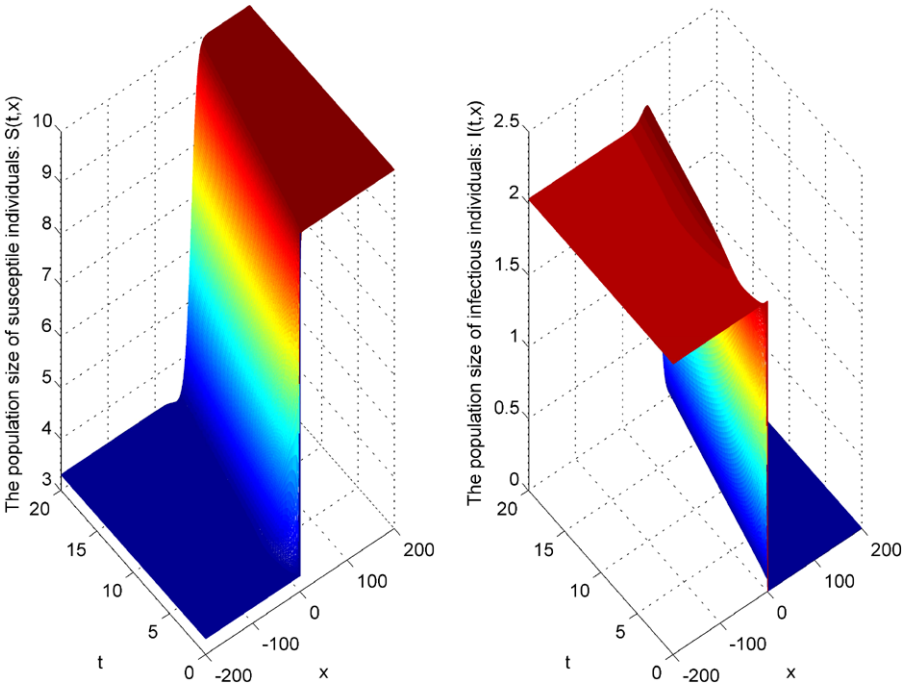

Fig. 9 The traveling wave observed in the system (20) with parameters: $\mu = 5$, $d = 0.5$, $r = 0.5$, $\sigma_L = \gamma_L = 0$, $\sigma = 0.25$, $\gamma = 0.25$, $D_S = 10$, $D_L = D_I = 10$ and $\tau = 1.0050$.

We point out that for convenience of computations, we choose mesh size Δt and time interval $[0, T]$ to be cooperative with the size of delay τ in the sense that $\tau/\Delta t$ is an integer. Details of the numeric method are described in Appendix A.2.

Figure 9 is the simulation result of (20) with (37) and $D_S = 10$, $D_L = D_I = 10$ and $\tau = 1.0050$, clearly showing that the disease geographically spreads at a speed approximately equal to $100/20 = 5.0$ (see the right sub-figure of Fig. 9) which is very close to 4.9974, the c^* value for parameters satisfying (36) and $\tau = 1$. Note that $\tau = 1.0050$ is very close to $\tau = 1$.

Still assuming (37) and $\tau = 1.0050$, but taking $D_S = 1$, $D_L = D_I = 1$, the numeric result is shown in Fig. 10. Note that the z^* determined by (34) is independent of the diffusion rates. Thus, in the case of $D_L = D_I$, by (35), when $D_I = D_L$ is decreased from 10 to 1, c^* is decreased by $1/\sqrt{10}$ times, the value of c^* for these set of parameter values should be $4.9974/\sqrt{10} \approx 1.58$, which seems to be the spread speed of the disease shown in Fig. 10 (from the right sub-figure).

Figure 11 aims at comparing the impact of latent length on the spread speed. All parameters are assumed the same as for Fig. 9 except that τ is doubled now to $\tau = 2.0101$. As the right sub-figure clearly shows, the spread speed is less than that in Fig. 9.

We also point out that there is a difference between wave profiles in Figs. 9–10 and Fig. 11 caused by the change of the length of latent delay: the first two have a hump in wave profile for ψ and a corresponding dip in that for ϕ, but the latter dose not seem to show these any more.

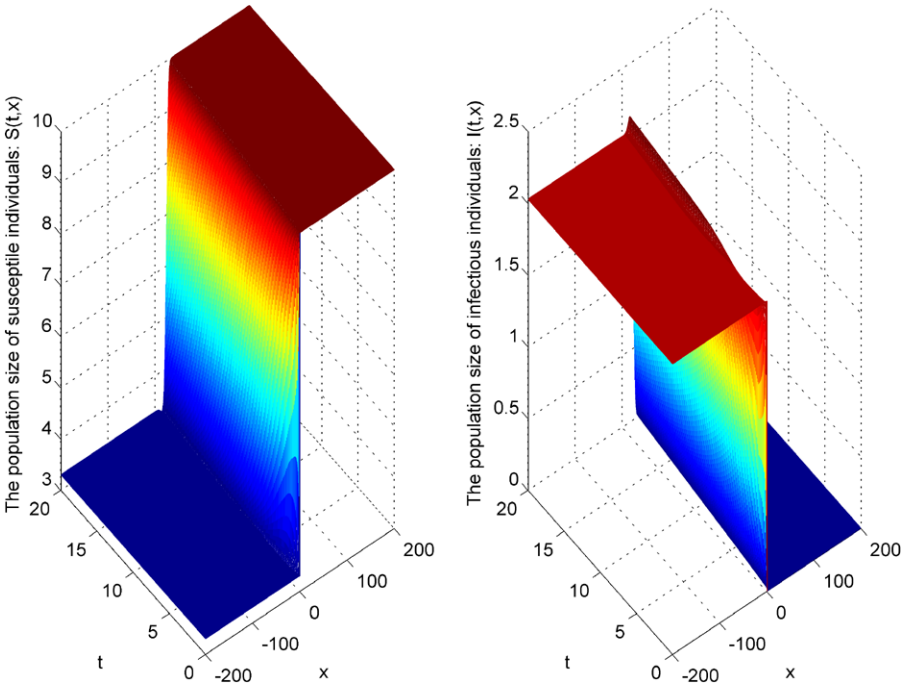

Fig. 10 The traveling wave observed in the system (20) with parameters: $\mu = 5$, $d = 0.5$, $r = 0.5$, $\sigma_L = \gamma_L = 0$, $\sigma = 0.25$, $\gamma = 0.25$, $D_S = 1$, $D_L = D_I = 1$ and $\tau = 1.0050$.

6. Conclusions and discussion

In this paper, we have derived a new epidemic model to describe the dynamics of diseases with a fixed latency carried and transmitted among the individuals living in a spatially continuous environment. Starting from the classical SIR model with a simple demographical structure, making use of a first-order linear partial differential equation for the evolution of diseases with infection age and time, and tracking the dispersal of latent individuals, we have obtained the model in the form of a system of delay reaction-diffusion equations, which in addition to the diffusion terms, contains a *non-local infection term*. The delay $\tau > 0$ represents the latency length of the disease. The non-local term reflects the mobility of the individuals during the latent period.

By an abstract treatment, we have established the existence, uniqueness, and positivity of the solution to the initial-value problem associated to this model system. Moreover, we have explored the existence of the traveling wave solutions for this system. We have derived a necessary condition that determines a critical value c^*, which serves at least as a lower bound for the wave speed in the sense that when $c < c^*$, there is no traveling wave front connecting the disease free equilibrium and the endemic equilibrium with the speed c. Although we are not able to prove that this c^* is the minimal wave speed, our numeric simulations of the wave equation seem to support the conjecture that it is the

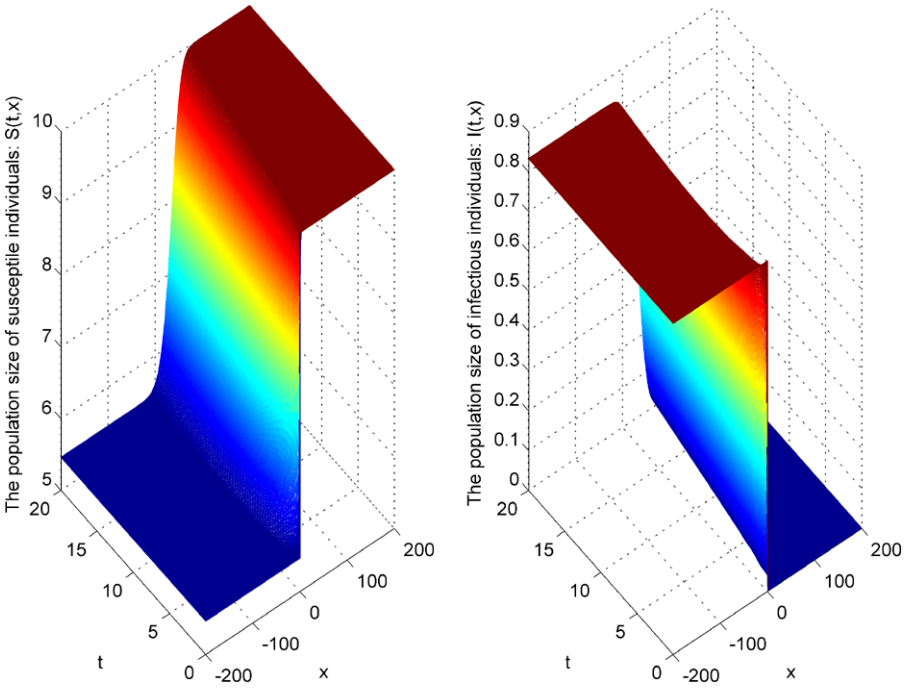

Fig. 11 The traveling wave observed in the system (20) with parameters: $\mu = 5$, $d = 0.5$, $r = 0.5$, $\sigma_L = \gamma_L = 0$, $\sigma = 0.25$, $\gamma = 0.25$, $D_S = 10$, $D_L = D_I = 10$ and $\tau = 2.0101$.

minimal wave speed. Furthermore, the numeric simulations to the original PDE model suggest that c^* is indeed also the spatial spread speed of the disease.

We have seen that c^* plays an important role in the disease spread described by the model (20). Some information about how the model parameters affect c^* is useful and helpful. For the case of $D_L = D_I$, the following properties can be easily obtained from (34) and (35):

(i) c^* is decreasing in τ;
(ii) c^* is decreasing in β;
(iii) c^* is increasing in $\epsilon r\mu/d$;
(iv) c^* is independent of D_S;
(v) c^* is proportional to $\sqrt{D_I} = \sqrt{D_L}$.

An immediate observation from (i) is that the latency may cause slow wave fronts. This is because for any given $c > 0$, there is a $\tau^* > 0$ such that when $\tau > \tau^*$, the corresponding $c^*(\tau) < c$, implying that the traveling wavefront with speed c becomes possible. For example, take parameter values used for numeric simulations resulted in Fig. 6. Then it is seen that for $c = 3$, there is no traveling wavefront with this speed. However, if we increase τ from $\tau = 1$ to $\tau = 2$, the corresponding $c^*(\tau) = c^*(2) = 2.8954 < 3$, and hence the model may have a traveling wavefront with speed $c = 3$, as is shown in the Fig. 12.

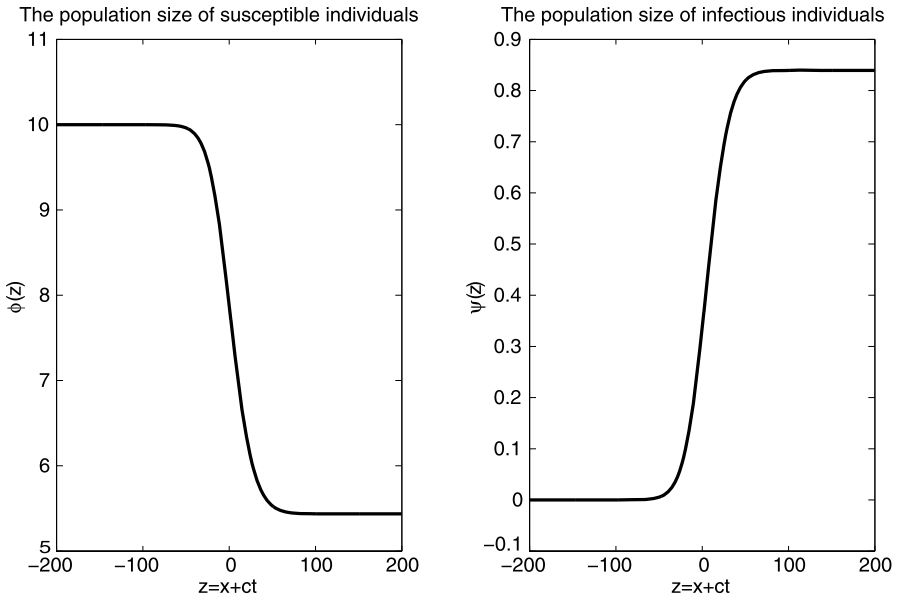

Fig. 12 Delay induced traveling wave fronts: simulation of (26) with parameters: $\mu = 5$, $d = 0.5$, $r = 0.5$, $\sigma_L = \gamma_L = 0$, $\sigma = 0.25$, $\gamma = 0.25$, $D_S = 10$, $D_L = D_I = 10$, $\tau = 2$ and $c = 3$.

We point out that delay induced traveling wave fronts have also been previously obtained (see, e.g., Zou, 2002).

As we mentioned above, the numeric results for the wave equation (26) seem to confirm that for every $c \geq c^*$, the model system (20) has a traveling wave front with speed c; however, the numeric results directly on (20) suggest that the actual spread speed of the disease coincide with c^*. The relation of minimal wave speed and the spread speed of a system is an interesting and important issue, and has attracted much attention recently. In their recent work Liang and Zhao (2007) have proved that for a class of systems with certain monotonicity, these two speeds indeed coincide. Our numeric results seem to have confirmed this conclusion for another class of system, not monotone though. Theoretical proofs of this conclusion for our model system, as well as for the existence of traveling wave fronts (usually these two topics are closely related; see, e.g., Liang and Zhao, 2007 and the references therein) remain interesting and challenging mathematical problems.

We also have seen that the length of the latent period affects the wave profile: for short latency, the wave profile tends to be non-monotone with a hump in the profile of infectious component and a corresponding dip in that of susceptible component, but these seem to disappear when the latency is longer. From this, we know that the longer the latency, the smaller the magnitude of the disease outbreak.

To conclude this section, we point out that the same idea can be applied to the situation where the spatial domain is bounded to derive similar models. The resulting models would have the same form as (20) but the kernel function $f_\alpha(x)$ will be given by an infinite series (instead of by an integral) and it depends on the boundary condition. For example, for the

one-dimensional domain $\Omega = [0, K]$, one can obtain the following model form:

$$\begin{cases} \dfrac{\partial S(t,x)}{\partial t} = \mu + D_S \dfrac{\partial^2 S(t,x)}{\partial x^2} - dS(t,x) - rI(t,x)S(t,x), \\ \dfrac{\partial I(t,x)}{\partial t} = D_I \dfrac{\partial^2 I(t,x)}{\partial x^2} - \beta I(t,x) \\ \qquad\qquad + \dfrac{\epsilon}{K} \displaystyle\int_0^K rI(t-\tau, y)S(t-\tau, y) f_\alpha(x, y)\, dy, \\ 0 < x < K,\ t > 0, \end{cases} \tag{38}$$

with initial conditions

$$S(t,x) = S_0(t,x), \quad I(t,x) = I_0(t,x), \quad \text{for } 0 < x < K,\ t \in [-\tau, 0]. \tag{39}$$

Here, if the homogeneous Dirichlet condition at $x = 0$ and K is proposed, then

$$f_\alpha(x,y) = \sum_{n=1}^{\infty} \left[\cos\frac{n\pi}{K}(x-y) - \cos\frac{n\pi}{K}(x+y) \right] e^{-(\frac{n\pi}{K})^2\alpha}, \tag{40}$$

and the following corresponding homogeneous Dirichlet condition should also be associated to (38)

$$S(t,0) = S(t,K) = 0, \quad I(t,0) = I(t,K) = 0, \quad \text{for } t \geq 0. \tag{41}$$

Similarly, if the homogeneous Neumann boundary condition is posed at $x = 0$ and K, we should have

$$f_\alpha(x,y) = 1 + \sum_{n=1}^{\infty} \left[\cos\frac{n\pi}{K}(x-y) + \cos\frac{n\pi}{K}(x+y) \right] e^{-(\frac{n\pi}{K})^2\alpha} \tag{42}$$

in (38) together with the following boundary condition:

$$S_x'(t,0) = S_x'(t,K) = 0, \quad I_x'(t,0) = I_x'(t,K) = 0, \quad \text{for } t \geq 0. \tag{43}$$

There may be other types of boundary conditions at $x = 0$ and K, resulting in different forms of $f_\alpha(x,y)$. The disease dynamics of models (38)–(39) with either (40)–(41) or (42)–(43) totally remains open. In particular, the basic reproduction number for such a model is a very interesting and appealing topic.

Appendix: Numeric methods

In this section, we give the details of the numeric methods based on which the numeric simulation results in Section 5 are obtained. Appendix A.1 is devoted to the numeric method for simulation of the wave equation (26) and the asymptotic boundary conditions (27), while Appendix A.2 describes the method that directly numerically solves the system (20).

Firstly, the wave equations (26) will be discussed by using the finite difference method coupled with the iterative technique. Secondly, the method of lines together with the finite difference method and iterative technique will be applied to the delayed partial differential system which includes E Eq. (1) with boundary condition (6) and S, I equations in (8).

A.1 Numerical method for (26) and (27)

The main idea is to use the finite difference method to obtain an algebraic system that approximates the wave equations (26). Since there is an integral term (non-local term) in the ψ equation in (26), the problem is not trivial, and thus, is worth of some detailed description for the reader's convenience.

Truncate $\mathbb{R} = (-\infty, \infty)$ by $[-K, K]$ where K is a very large number. Take the uniform partition of domain $[-K, K]$:

$$-K = z_1 < z_2 < \cdots < z_{2n-1} < z_{2n} < z_{2n+1} = K$$

where $h = 2K/2n = K/n$ and $z_i = z_1 + (i-1)h$, $i = 1, 2, \ldots, 2n+1$. Corresponding to the truncation, the asymptotic boundary conditions in (27) are then translated to

$$\phi(z_1) = \frac{\mu}{d}, \qquad \phi(z_{2n+1}) = \frac{\beta}{r\epsilon}, \quad \text{and} \quad \psi(z_1) = 0, \quad \psi(z_{2n+1}) = \frac{\mu\epsilon}{\beta} - \frac{d}{r}. \tag{A.1}$$

Following the conventional numeric differentiation, the differential operators in the wave equations can be approximated by

$$\begin{cases} \phi'(z_i) = \dfrac{\phi(z_i) - \phi(z_{i-1})}{h} + O(h), \\ \phi''(z_i) = \dfrac{\phi(z_{i+1}) - 2\phi(z_i) + \phi(z_{i-1})}{h^2} + O\big(h^2\big), \\ \psi'(z_i) = \dfrac{\psi(z_i) - \psi(z_{i-1})}{h} + O(h), \\ \psi''(z_i) = \dfrac{\psi(z_{i+1}) - 2\psi(z_i) + \psi(z_{i-1})}{h^2} + O\big(h^2\big). \end{cases} \tag{A.2}$$

By the above (A.2), the ϕ equation in (26) is immediately discretized to

$$c\frac{\phi(z_i) - \phi(z_{i-1})}{h} = \mu + D_S\frac{\phi(z_{i+1}) - 2\phi(z_i) + \phi(z_{i-1})}{h^2} - d\phi(z_i) - r\phi(z_i)\psi(z_i),$$

which is rewritten as

$$\begin{aligned} &(D_S + ch)\phi(z_{i-1}) - \big(2D_S + dh^2 + ch\big)\phi(z_i) + D_S\phi(z_{i+1}) \\ &\quad - rh^2\phi(z_i)\psi(z_i) + \mu h^2 = 0. \end{aligned} \tag{A.3}$$

For the ψ equation in (26), the local portion can be similarly discretized, but the integral term needs some work. We first notice that

$$\epsilon \int_{-\infty}^{+\infty} r\phi(z-y-c\tau)\psi(z-y-c\tau) f_\alpha(y)\,dy$$
$$= \epsilon r \int_{-\infty}^{+\infty} \phi(y)\psi(y) f_\alpha(z-y-c\tau)\,dy.$$

Using the large number K, we split the integral over $(-\infty, +\infty)$ into three over the intervals: $(-\infty, -K]$, $[-K, K]$, and $[K, \infty)$. Observe that

$$\int_{-\infty}^{-K} \phi(y)\psi(y) f_\alpha(z-y-c\tau)\,dy \approx \int_{-\infty}^{-K} \phi(-K)\psi(-K) f_\alpha(z-y-c\tau)\,dy,$$

which could be arbitrary small by taking K sufficiently large (since $\psi(-\infty) = 0$). Also note that

$$\int_{K}^{+\infty} \phi(y)\psi(y) f_\alpha(z-y-c\tau)\,dy = \int_{K}^{+\infty} \phi(K)\psi(K) f_\alpha(z-y-c\tau)\,dy$$
$$= \phi(z_{2n+1})\psi(z_{2n+1}) \int_{K}^{+\infty} f_\alpha(z-y-c\tau)\,dy.$$

These give the following approximation:

$$\int_{-\infty}^{+\infty} \phi(y)\psi(y) f_\alpha(z-y-c\tau)\,dy$$
$$\approx \int_{-K}^{K} \phi(y)\psi(y) f_\alpha(z-y-c\tau)\,dy$$
$$+ \phi(z_{2n+1})\psi(z_{2n+1}) \int_{K}^{+\infty} f_\alpha(z-y-c\tau)\,dy. \tag{A.4}$$

For the first term on the right-hand side of (A.4), we use the composite Simpson's rule to obtain

$$\int_{-K}^{K} \phi(y)\psi(y) f_\alpha(z_i-y-c\tau)\,dy$$
$$= \frac{h}{3}\big\{\phi(z_1)\psi(z_1) f_\alpha(z_i-z_1-c\tau)$$
$$+ 4\big[\phi(z_2)\psi(z_2) f_\alpha(z_i-z_2-c\tau) + \phi(z_4)\psi(z_4) f_\alpha(z_i-z_4-c\tau) + \cdots$$
$$+ \phi(z_{2n-2})\psi(z_{2n-2}) f_\alpha(z_i-z_{2n-2}-c\tau) + \phi(z_{2n})\psi(z_{2n}) f_\alpha(z_i-z_{2n}-c\tau)\big]$$
$$+ 2\big[\phi(z_3)\psi(z_3) f_\alpha(z_i-z_3-c\tau) + \phi(z_5)\psi(z_5) f_\alpha(z_i-z_5-c\tau)$$
$$+ \cdots + \phi(z_{2n-3})\psi(z_{2n-3}) f_\alpha(z_i-z_{2n-3}-c\tau)$$
$$+ \phi(z_{2n-1})\psi(z_{2n-1}) f_\alpha(z_i-z_{2n-1}-c\tau)\big]$$

$$
\begin{aligned}
&+\phi(z_{2n+1})\psi(z_{2n+1})f_\alpha(z_i - z_{2n+1} - c\tau)\Big\} \\
&= \frac{h}{3}\Bigg(\phi(z_1)\psi(z_1)f_\alpha(z_i - z_1 - c\tau) + 4\sum_{j=1}^{n}\phi(z_{2j})\psi(z_{2j})f_\alpha(z_i - z_{2j} - c\tau) \\
&\quad + 2\sum_{j=1}^{n}\phi(z_{2j+1})\psi(z_{2j+1})f_\alpha(z_i - z_{2j+1} - c\tau) \\
&\quad + \phi(z_{2n+1})\psi(z_{2n+1})f_\alpha(z_i - z_{2n+1} - c\tau)\Bigg). \qquad \text{(A.5)}
\end{aligned}
$$

For the second term on the right-hand side of (A.4), we have the following:

$$
\int_K^{+\infty} f_\alpha(z_i - y - c\tau)\,dy = \int_{-\infty}^{z_i - K - c\tau} f_\alpha(y)\,dy = \frac{1}{2}\Bigg(1 - \int_{z_i - K - c\tau}^{K + c\tau - z_i} f_\alpha(y)\,dy\Bigg). \qquad \text{(A.6)}
$$

With the above preparation, the ψ equation in (26) is then discretized to

$$
\begin{aligned}
c\frac{\psi(z_i) - \psi(z_{i-1})}{h} &= D_I\frac{\psi(z_{i+1}) - 2\psi(z_i) + \psi(z_{i-1})}{h^2} - \beta\psi(z_i) \\
&\quad + \frac{\epsilon r h}{3}\Bigg(\phi(z_1)\psi(z_1)f_\alpha(z_i - z_1 - c\tau) \\
&\quad + 4\sum_{j=1}^{n}\phi(z_{2j})\psi(z_{2j})f_\alpha(z_i - z_{2j} - c\tau) \\
&\quad + 2\sum_{j=1}^{n}\phi(z_{2j+1})\psi(z_{2j+1})f_\alpha(z_i - z_{2j+1} - c\tau) \\
&\quad + \phi(z_{2n+1})\psi(z_{2n+1})f_\alpha(z_i - z_{2n+1} - c\tau)\Bigg) \\
&\quad + \frac{\epsilon r}{2}\phi(z_{2n+1})\psi(z_{2n+1})\Bigg(1 - \int_{z_i - z_{2n+1} - c\tau}^{z_{2n+1} + c\tau - z_i} f_\alpha(y)\,dy\Bigg),
\end{aligned}
$$

which is equivalently rewritten as

$$
\begin{aligned}
&(D_I + ch)\psi(z_{i-1}) - \big(2D_I + \beta h^2 + ch\big)\psi(z_i) + D_I\psi(z_{i+1}) \\
&\quad + \frac{\epsilon r h^3}{3}\Bigg(\phi(z_1)\psi(z_1)f_\alpha(z_i - z_1 - c\tau) \\
&\quad + 4\sum_{j=1}^{n}\phi(z_{2j})\psi(z_{2j})f_\alpha(z_i - z_{2j} - c\tau)
\end{aligned}
$$

$$+2\sum_{j=1}^{n}\phi(z_{2j+1})\psi(z_{2j+1})f_\alpha(z_i-z_{2j+1}-c\tau)$$

$$+\phi(z_{2n+1})\psi(z_{2n+1})f_\alpha(z_i-z_{2n+1}-c\tau)\Bigg)$$

$$+\frac{\epsilon r h^2}{2}\phi(z_{2n+1})\psi(z_{2n+1})\left(1-\int_{z_i-z_{2n+1}-c\tau}^{z_{2n+1}+c\tau-z_i}f_\alpha(y)\,dy\right)=0. \tag{A.7}$$

Equations (A.3) and (A.7) form an algebraic system, the solution of which, gives the values of the numeric solution of (26) on all mesh points z_i, $i=1,2,\ldots,2n+1$. For convenience of using softwares such as Matlab, Maple, or Mathematica, we next rewrite this system in matrix form. For (A.7), we have

$$\mathbf{M}_1\begin{bmatrix}\psi(z_1)\\ \psi(z_2)\\ \vdots\\ \psi(z_{2n})\\ \psi(z_{2n+1})\end{bmatrix}+\mathbf{N}_1\begin{bmatrix}\phi(z_1)\psi(z_1)\\ \phi(z_2)\psi(z_2)\\ \vdots\\ \phi(z_{2n})\psi(z_{2n})\\ \phi(z_{2n+1})\psi(z_{2n+1})\end{bmatrix}+\mathbf{C}_1=0, \tag{A.8}$$

where

$$\mathbf{M}_1=\begin{bmatrix}1 & 0 & 0 & \cdots & 0\\ D_I+ch & -(\beta h^2+ch+2D_I) & D_I & \cdots & 0\\ \vdots & \ddots & \ddots & \ddots & \vdots\\ 0 & \cdots & D_I+ch & -(\beta h^2+ch+2D_I) & D_I\\ 0 & 0 & \cdots & 0 & 1\end{bmatrix},$$

and

$$\mathbf{N}_1=\frac{\epsilon r h^3}{3}\begin{bmatrix}0 & 0 & 0 & \cdots & 0\\ f_\alpha(z_{2,1}-c\tau) & 4f_\alpha(z_{2,2}-c\tau) & 2f_\alpha(z_{2,3}-c\tau) & \cdots & f_\alpha(z_{2,2n+1}-c\tau)\\ \vdots & \vdots & \vdots & \vdots & \vdots\\ f_\alpha(z_{2n,1}-c\tau) & f_\alpha(z_{2n,2}-c\tau) & f_\alpha(z_{2n,3}-c\tau) & \cdots & f_\alpha(z_{2n,2n+1}-c\tau)\\ 0 & 0 & 0 & \cdots & 0\end{bmatrix},$$

with $f_\alpha(z_{i,j}-c\tau)=f_\alpha(z_i-z_j-c\tau)$, and

$$\mathbf{C}_1=\begin{bmatrix}0\\ \frac{\epsilon r h^2}{2}\phi(z_{2n+1})\psi(z_{2n+1})\left(1-\int_{z_2-z_{2n+1}-c\tau}^{z_{2n+1}+c\tau-z_2}f_\alpha(y)\,dy\right)\\ \vdots\\ \frac{\epsilon r h^2}{2}\phi(z_{2n+1})\psi(z_{2n+1})\left(1-\int_{z_{2n}-z_{2n+1}-c\tau}^{z_{2n+1}+c\tau-z_{2n}}f_\alpha(y)\,dy\right)\\ -\left(\frac{\mu\epsilon}{\beta}-\frac{d}{r}\right)\end{bmatrix}.$$

For (A.3), we have

$$\mathbf{M}_2\begin{bmatrix}\phi(z_1)\\ \phi(z_2)\\ \vdots\\ \phi(z_{2n})\\ \phi(z_{2n+1})\end{bmatrix}+\mathbf{N}_2\begin{bmatrix}\phi(z_1)\psi(z_1)\\ \phi(z_2)\psi(z_2)\\ \vdots\\ \phi(z_{2n})\psi(z_{2n})\\ \phi(z_{2n+1})\psi(z_{2n+1})\end{bmatrix}+\mathbf{C}_2=0, \tag{A.9}$$

where

$$\mathbf{M}_2=\begin{bmatrix}1 & 0 & 0 & \cdots & 0\\ D_S+ch & -(dh^2+ch+2D_S) & D_S & \cdots & 0\\ \vdots & \ddots & \ddots & \ddots & \vdots\\ 0 & \cdots & D_S+ch & -(dh^2+ch+2D_S) & D_S\\ 0 & \cdots & 0 & 0 & 1\end{bmatrix},$$

$$\mathbf{N}_2=\begin{bmatrix}0 & 0 & \cdots & 0 & 0\\ 0 & -rh^2 & \cdots & 0 & 0\\ \vdots & \vdots & \ddots & \vdots & \vdots\\ 0 & 0 & \cdots & -rh^2 & 0\\ 0 & 0 & \cdots & 0 & 0\end{bmatrix},\quad \text{and}\quad \mathbf{C}_2=\begin{bmatrix}-\frac{\mu}{d}\\ \mu h^2\\ \vdots\\ \mu h^2\\ -\frac{\beta}{r\epsilon}\end{bmatrix}.$$

Finally, let $\mathbf{w}=[w(1),\ldots,w(2n+1),w(2n+2),\ldots,w(4n+2)]^T\in\mathbb{R}^{4n+2}$ be defined by

$$w(i)=\begin{cases}\psi(i), & \text{for } 1\le i\le 2n+1,\\ \phi(i-2n-1), & \text{for } 2n+1<i\le 4n+2.\end{cases}$$

Then the algebraic system is rewritten as the following matrix form:

$$\begin{bmatrix}\mathbf{M}_1 & 0\\ 0 & \mathbf{M}_2\end{bmatrix}\begin{bmatrix}w(1)\\ \vdots\\ w(2n+1)\\ w(2n+2)\\ \vdots\\ w(4n+2)\end{bmatrix}+\begin{bmatrix}\mathbf{N}_1 & 0\\ 0 & \mathbf{N}_2\end{bmatrix}\begin{bmatrix}w(2n+2)w(1)\\ \vdots\\ w(4n+2)w(2n+1)\\ w(1)w(2n+2)\\ \vdots\\ w(2n+1)w(4n+2)\end{bmatrix}+\begin{bmatrix}\mathbf{C}_1\\ \mathbf{C}_2\end{bmatrix}=\mathbf{0}. \tag{A.10}$$

This is the matrix form for algebraic system we implemented on Matlab to obtain the numeric results given in Section 5.

A.2 Numerical method for (20)

The method of lines is very useful in solving a reaction diffusion system in the absence of time delay and spatial non-locality. By discretizing the spatial variable x, the method

firstly transfers the R-D system into a system of ordinary differential equations on the spatial grid points. Then by any ODE solver, the resulting ODE system is solved, giving numeric solutions showing evolution with respect to time variable on the spatial grid points. But our model (20) contains a time delay representing latent period as well as a non-local term resulted from the mobility of the latent individuals; the method can not be applied directly. However, based on the feature of our model, we find that as far as numeric solutions of (20) are concerned, we can actually transform this system into one without non-locality. The details are given below.

Note that (20) and its initial conditions can be described by

$$\begin{cases} \dfrac{\partial S(t,x)}{\partial t} = \mu + D_S \dfrac{\partial^2 S(t,x)}{\partial x^2} - dS(t,x) - rI(t,x)S(t,x), \quad x \in \mathbb{R}, t \geq 0, \\ \dfrac{\partial I(t,x)}{\partial t} = D_I \dfrac{\partial^2 I(t,x)}{\partial x^2} - \beta I(t,x) + E(t,\tau,x), \quad x \in \mathbb{R}, t \geq 0, \\ S(t,x) = \phi_S(t,x), \quad I(t,x) = \phi_I(t,x), \quad x \in \mathbb{R}, t \in [-\tau, 0], \end{cases} \tag{A.11}$$

where $E(t,\tau,x)$ is determined by

$$\begin{cases} \dfrac{\partial E(t,a,x)}{\partial t} + \dfrac{\partial E(t,a,x)}{\partial a} = D_L \dfrac{\partial^2 E(t,a,x)}{\partial x^2} - \bar{d} E(t,a,x), \\ \quad x \in \mathbb{R}, t \geq 0, a \in [0,\tau], \\ E(t,0,x) = rS(t,x)I(t,x). \end{cases} \tag{A.12}$$

Now, observe that for any fixed $t \geq 0$, $E(t,\tau,x) = u(t,s,x)|_{s=\tau}$ where $u(t,s,x)$ is the solution of the following initial value problem

$$\begin{cases} \dfrac{\partial u(t,s,x)}{\partial s} = D_L \dfrac{\partial^2 u(t,s,x)}{\partial x^2} - \bar{d} u(t,s,x), \quad x \in \mathbb{R}, s \geq 0, \\ u(t,0,x) = rS(t-\tau,x)I(t-\tau,x). \end{cases} \tag{A.13}$$

Now, truncate $\mathbb{R} = (-\infty, \infty)$ by $[-K, K]$ and take the uniform partition of $[-K, K]$ by

$$-K = x_1 < x_2 < \cdots < x_{n-1} < x_n = K,$$

with $x_i = x_1 + (i-1)\Delta x$ and $\Delta x = 2L/(n-1)$. Adopting the second-order central difference operator to approximate the second order partial derivative with respect to the spatial variable x, (A.11) respectively discretized to

$$\begin{cases} \dfrac{\partial S(t,x_i)}{\partial t} = \mu + D_S \dfrac{S(t,x_{i+1}) - 2S(t,x_i) + S(t,x_{i-1})}{(\Delta x)^2} \\ \qquad\qquad - dS(t,x_i) - rI(t,x_i)S(t,x_i), \quad t \geq 0, \\ \dfrac{\partial I(t,x_i)}{\partial t} = D_I \dfrac{I(t,x_{i+1}) - 2I(t,x_i) + I(t,x_{i-1})}{(\Delta x)^2} - \beta I(t,x_i) + u(t,\tau,x_i), \\ \quad t \geq 0, \end{cases} \tag{A.14}$$

with the initial conditions:

$$S(t, x_i) = \phi_S(t, x_i), \quad I(t, x_i) = \phi_I(t, x_i), \quad t \in [-\tau, 0], \tag{A.15}$$

and (A.13) is discretized to

$$\begin{cases} \dfrac{\partial u(t, s, x_i)}{\partial s} = D_L \dfrac{u(t, s, x_{i+1}) - 2u(t, s, x_i) + u(t, s, x_{i-1})}{(\Delta x)^2} - \bar{d}u(t, s, x_i), \\ s \geq 0, \\ u(t, 0, x_i) = rS(t - \tau, x_i) I(t - \tau, x_i). \end{cases} \tag{A.16}$$

Here, we use the homogeneous Neumann boundary conditions at $x_1 = -K$ and $x_n = K$ for both (A.14) and (A.16).

Let $[0, T]$ be the time interval on which one would like to obtain the numeric solutions. Take the uniform partition of $[0, T]$:

$$0 = t_1 < t_2 < \cdots < t_{N-1} < t_N = T,$$

where $t_i = (i - 1)\Delta t$ with $\Delta t = T/(N - 1)$. One can always choose T and Δt to be "cooperative" with the time delay τ in the sense that $\tau/\Delta t$ is an integer. Now we are ready to solve the system (A.16) and (A.14) in an iterative and inductive way, as described below.

Firstly, by using the initial values of S and I given in (A.15), we can solve the equation ODE system (A.16) for $u(0, s, x)$ for $s \in [0, \tau]$, yielding the value $u(t_1, \tau, x_i) = u(0, \tau, x_i)$. Secondly, for $t \in [t_1, t_2] = [0, \Delta t]$, approximate $u(t, \tau, x_i)$ by $u(t_1, \tau, x_i)$ and solve (A.14) with $u(t, \tau, x_i)$ being replaced by $u(t_1, \tau, x_i)$, one may obtain the values of $S(t, x_i)$ and $I(t, x_i)$ for $t \in [t_1, t_2]$, completing one round of cross iteration. The above process can be repeated, starting with (A.16) again but with $t = t_2$, and then moving to (A.14) for $t \in [t_2, t_3]$. Inductively, the iteration can be continued until $t \in [t_{N-1}, t_N]$.

References

Anderson, R.M., Trewhella, W.J., 1985. Population dynamics of the badger (Meles meles) and the epidemiology of bovine tuberculosis (mycobacterium bovis). Philos. Trans. R. Soc. Lond. B 310, 327–381.

Arino, J., van den Driessche, P., 2003a. A multi-city epidemic model. Math. Popul. Stud. 10, 175–193.

Arino, J., van den Driessche, P., 2003b. The basic reproduction number in a multi-city compartmental epidemic model. LNCIS 294, 135–142.

Arino, J., van den Driessche, P., 2006. Metapopulation epidemic models, a survey. Fields Inst. Commun. 48, 1–12.

Barlow, N.D., 2000. Non-linear transmission and simple models for bovine tuberculosis. J. Anim. Ecol. 69, 703–713.

Brauer, F., van den Driessche, P., 2001. Models for transmission of disease with immigration of infectives. Math. Biosci. 171, 143–154.

Brauer, F., van den Driessche, P., Wu, J., 2008. Mathematical Epidemiology. Lecture Notes in Mathematics. Springer, Berlin/Heidelberg.

Castillo-Chavez, C., Yakubu, A.A., 2001. Dispersal, disease and life-history evolution. Math. Biosci. 173, 35–53.

Daners, D., Medina, P.K., 1992. Abstract evolution equations, periodic problems and applications. In: Pitman Research Notes in Mathematics, vol. 279. Longman, Harlow.

Dunbar, S., 1981. Travelling wave solutions of diffusive Lotka–Volterra interaction equations. Ph.D. thesis, Univ. Minnesota, Minneapolis.
Dunbar, S., 1983. Travelling wave solutions of diffusive Lotka–Volterra equations. J. Math. Biol. 17, 11–32.
Dunbar, S., 1984. Traveling wave solutions of diffusive Lotka–Volterra equations: a heteroclinic connection in R^4. Trans. Am. Math. Soc. 286, 557–594.
Gardner, R.A., 1984. Existence of travelling wave solutions of predator-prey systems via the connection index. SIAM J. Appl. Math. 44, 56–79.
Garnett, B.T., Delahay, R.J., Roper, T.J., 2002. Use of cattle farm resources by badgers (Meles meles) and risk of bovine tuberculosis (mycobacterium bovis) transmission to cattle. Proc. R. Soc. B 269, 1487–1491.
Hethcote, H.W., 2000. The mathematics of infectious diseases. SIAM Rev. 42, 599–653.
Hsieh, Y.-H., van den Driessche, P., Wang, L., 2007. Impact of travel between patches for spatial spread of disease. Bull. Math. Biol. 69, 1355–1375.
Huang, J., Lu, G., Ruan, S., 2003. Existence of traveling wave solutions in a diffusive predator-prey model. J. Math. Biol. 46, 132–152.
Li, J., Zou, X., 2009a. Generalization of the Kermack-McKendrick SIR model to a patchy environment for a disease with latency. Math. Model. Nat. Phenom. 4(2), 92–118.
Li, J., Zou, X., 2009b. An epidemic model with non-local infections on a patchy environment. J. Math. Biol. doi:10.1007/s00285-009-0280-9, in press.
Liang, X., Zhao, X.-Q., 2007. Asymptotic speeds of spread and traveling waves for monotone semiflows with applications. Commun. Pure Appl. Math. 60, 1–40.
Martin Jr, R.H., Smith, H.L., 1990. Abstract functional-differential equations and reaction-diffusion systems. Trans. Am. Math. Soc. 321, 1–44.
Metz, J.A.J., Diekmann, O. (Eds.), 1986. The Dynamics of Physiologically Structured Populations. Springer, New York.
Murray, J.D., 2002. Mathematical Biology, 3rd edn. Springer, New York.
Salmani, M., van den Driessche, P., 2006. A model for disease transmission in a patchy environment. Discrete Contin. Dyn. Syst. B 6, 185–202.
Thoen, C.O., Karlson, A.G., Himes, E.M., 1984. Mycobacterium tuberculosis complex. In: The Mycobacteria, A Sourcebook, pp. 1209–1235. Dekker, New York.
van den Driessche, P., Wang, L., Zou, X., 2007. Modelling disease with latency and replase. Math. Biosci. Eng. 4, 205–219.
Wang, W., Mulone, G., 2003. Threshold of disease transmission on a patch environment. J. Math. Anal. Appl. 285, 321–335.
Wang, W., Zhao, X.-Q., 2004. An epidemic model in a patchy environment. Math. Biosci. 190, 97–112.
Wang, W., Zhao, X.-Q., 2005. An age-structured epidemic model in a patchy environment. SIAM J. Appl. Math. 65, 1597–1614.
Wang, W., Zhao, X.-Q., 2006. An epidemic model with population dispersal and infection period. SIAM J. Appl. Math. 66, 1454–1472.
Wu, J., 1996. Theory and Applications of Partial Functional Differential Equations. Applied Mathematical Science, vol. 119. Springer, Berlin.
Wu, J., Zou, X., 2001. Traveling wave fronts of reaction-diffusion systems with delay. J. Dyn. Differ. Equ. 13, 651–687.
Zou, X., 2002. Delay induced traveling wave fronts in reaction diffusion equations of KPP-Fisher type. J. Comput. Appl. Math. 146, 309–321.